Groundwater for Sustainable Development 28 (2025) 101389

Contents lists available at ScienceDirect

Groundwater for Sustainable Development

journal homepage: www.elsevier.com/locate/gsd

Research paper

Investigating the role of ENSO in groundwater temporal variability across Abu Dhabi Emirate, United Arab Emirates using machine learning algorithms

Khaled Alghafli [a,b,c,*], Xiaogang Shi [d], William Sloan [b], Awad M. Ali [e,f]

[a] Department of Civil and Environmental Engineering, Faculty of Engineering, United Arab Emirates, Al Ain, P.O. Box 15551, United Arab Emirates
[b] James Watt School of Engineering, University Glasgow, United Kingdom
[c] National Water and Energy Center, United Arab Emirates University, Al Ain, P.O. Box 15551, United Arab Emirates
[d] School of Social and Environmental Sustainability, University of Glasgow, Dumfries, United Kingdom
[e] Hydrology and Environmental Hydraulics Group, Wageningen University, P.O. BOX 47, 6700AA, Wageningen, the Netherlands
[f] Water Research Center, Faculty of Engineering, University of Khartoum, P.O. BOX 321, Khartoum, Sudan

HIGHLIGHTS

- Groundwater level predictions using LSTM and RF models achieved satisfactory accuracy across Abu Dhabi Emirate.
- Incorporating time lags improved the models' accuracy for groundwater level predictions.
- Global sensitivity analysis approach assessed the impact of input data on the model performance.

GRAPHICAL ABSTRACT

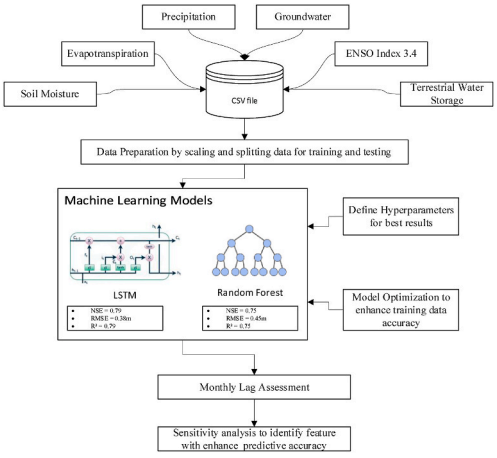

ARTICLE INFO

Keywords:
Groundwater level
Machine learning
Random forest
LSTM
Sensitivity analysis
El Niño-Southern oscillation

ABSTRACT

Accurate prediction of groundwater levels is crucial for managing groundwater resources efficiently. The complex aquifer heterogeneity and groundwater abstraction variation present challenges to have accurate groundwater level models over Abu Dhabi emirate, United Arab Emirates. In the present study, two data-driven models are employed, which are the Long Short-Term Memory (LSTM) and the Random Forest (RF) to develop a model for the prediction of monthly groundwater level in the Abu Dhabi Emirate. The incorporated data in the models are precipitation, terrestrial water storage, soil moisture, evapotranspiration, and the El Niño-Southern

* Corresponding author. Department of Civil and Environmental Engineering, Faculty of Engineering, United Arab Emirates, Al Ain P.O. Box 15551, United Arab Emirates.
E-mail address: khledalghafli@uaeu.ac.ae (K. Alghafli).

https://doi.org/10.1016/j.gsd.2024.101389
Received 19 August 2024; Received in revised form 23 November 2024; Accepted 1 December 2024
Available online 3 December 2024

Oscillation (ENSO) 3.4 index. The groundwater monitoring wells data are obtained for 263 monitoring wells distributed over Abu Dhabi emirate for the period 2000–2023 in a monthly temporal scale. The models' performance was assessed using the Nash-Sutcliffe efficiency (NSE), root mean square error (RMSE) the coefficient of determination (R^2) and Percent bias (PBIAS). An optimization technique was also applied to address the impact of the lags on enhancing the groundwater level model. The LSTM model outperformed the RF model during the testing period, achieving $R^2 = 0.79$, NSE = 0.70, RMSE = 0.38 m and PBIAS = 0.2% with a 3-month lag. The global sensitivity analysis was applied to understand the importance of each parameter and its influence on the models' output. This study highlights the potential use of data-driven models for the prediction of groundwater level which could aid water managers to monitor the groundwater resources at a regional scale. The developed model can serve as an alternative approach for predicting groundwater level change over the Abu Dhabi Emirate.

1. Introduction

The dynamic of groundwater storage change is challenging to understand owing to the numerous factors influencing its fluctuation (Alley et al., 2002; Dangar et al., 2021). Accurate estimation of groundwater level change is crucial for sustainably managing groundwater resources. The high depletion rate and drawdown in groundwater level is caused due to the global population growth and the increase in water demands from the industrial and agricultural sectors (Long et al., 2020). The groundwater abstraction is estimated to account for 25%–33% of the total withdrawals in the world (Döll et al., 2012; Hanasaki et al., 2018; Taylor et al., 2013). Thus, groundwater sustainable management is vital since aquifers provide 50% of the global drinking water supply and 43% of the world's irrigation (Siebert et al., 2010; Smith et al., 2016).

Depletion or overexploitation occurs when the rate of abstraction surpasses the recharge rate (Gleeson et al., 2010). The majority of aquifers are experiencing a severe groundwater level decline (Ali et al., 2020; Shamsudduha and Taylor, 2020; Wada et al., 2010), alarming many water managers to furtherly understand the dynamic of the aquifer systems and its response to climate change for the purpose of sustainable groundwater management. This decline will lead to several environmental issues, such as saltwater intrusion, land subsidence and the deterioration of water quality (Gong et al., 2020; O'Reilly et al., 2020; Su et al., 2017).

Arid and semi-arid regions are vulnerable to a water deficit to meet the water demand, given the limited rainfall events to recharge the groundwater aquifers (Huang et al., 2015). This has been noticed in several aquifers where the depletion rate reached 40 mm/year in north-western India and 27.6 mm/year in the high plains, USA and 22 mm/year in the North China Plain (Feng et al., 2013; Rodell et al., 2009; Scanlon et al., 2012). Various studies have addressed the approaches that should be adopted for sustainable water resources management. The common conclusion from all studies emphasized the importance to accurately simulate and quantify the groundwater level changes for achieving a sustainable management for groundwater resources (Gao et al., 2022; Samani et al., 2022; Yin et al., 2021).

Groundwater dynamics have been modeled using a conceptual (De Filippis et al., 2020) and physical models for the purpose of predicting the groundwater level (Boughriba and Jilali, 2018; El Yaouti et al., 2008). Although conceptual models require fewer data and parameters, it has limitation on providing detailed information over the studied area (De Filippis et al., 2020; Izady et al., 2014). Common numerical models, such as, MODFLOW (Harbaugh, 2005), FEFLOW (Diersch, 2014) and HydrGeoSphere (Brunner and Simmons, 2012) are used for the simulation of groundwater flow and could have limitations and uncertainties when observation data are scarce, particularly in the case of transient model, due to its process nature on oversimplifying the dynamic of physical process and the extensive data required (Sikdar, 2019; Wunsch et al., 2021b).

Usually, observation data collected manually or from telemetric devices suffers with outliers and gaps in the timeseries due to signal loss and battery failures in the telemetric devices leading to errors and uncertainty (Oikonomou et al., 2018). Consequently, developing transient numerical models may also experience large uncertainty since these temporal gaps within the datasets are filled using imputation techniques such as regression approaches (Cooley and Naff, 1990; Salas, 1980, 1993), interpolation techniques (Sorensen et al., 2021; Wunsch et al., 2022), machine learning techniques (Dax and Zilberbrand, 2018; Dwivedi et al., 2022). Additionally, the uneven distribution of observation data will require the use of spatial interpolation methods for the conversions of point data (e.g. precipitation station and groundwater monitoring well) to areal (Khazaz et al., 2015; Yao et al., 2014) which could lead to another source of uncertainty in the case of developing a regional scale model. The accuracy of interpolated data depends on the size of the study area and the spacing between the observation points data.

Furthermore, physically based models require extensive geological and hydrological data for setting boundary conditions which are not cost effective and time consuming (Di Nunno and Granata, 2020; Gupta et al., 2003). Factors like the nonlinearity of the governing groundwater flow equation, the complexity of the aquifer geology, and the spatial variation of rainfall patterns and aquifer characteristics along with the inconsistency of the human abstractions and recharge, contribute to a large source of errors when simulating the groundwater flow. It worths mentioning that the illegal abstraction from unregistered wells and water pipe network leakage to groundwater could result in errors during the calibration process of physical models (Al-Bakri, 2016; Gropius et al., 2022; Khaledi-Alamdari et al., 2022). All the discussed factors could negatively impact the calibration process and sensitivity analysis for these physical models where it could be biased to certain parameters causing a discrepancy in the model (Højberg and Refsgaard, 2005; Masafu and Williams, 2024; Rojas et al., 2008).

The exponential growth in the satellite industry resulted in the availability of remote sensing products with large data freely accessible to researchers. This growth paved the way for the application of Artificial Intelligence (AI) technology in the hydrology field. Machine learning approaches which is a data-driven technique is a branch of AI and has been applied for the prediction of groundwater level (Sahoo and Jha, 2013; Sahoo et al., 2017; Solgi et al., 2021; Tao et al., 2022; Wang et al., 2018; Wunsch et al., 2021b). Machine learning techniques identify the patterns hidden in historical data and learn from these patterns to predict the future changes and scenarios without exhaustive hydrological parameters knowledge.

Several studies assessed and compared physically based models with models developed from machine learning methods (Almuhaylan et al., 2020; Chen et al., 2020; Coppola et al., 2003; Mohammadi, 2008; Nikolos et al., 2008; Parkin et al., 2007) and concluded that data driven models outperformed physical models. Some machine learning models require hydrological and meteorological parameters coupled with the anthropogenic practice data (e.g. irrigation rate, land cover, service population and dams) as an input for predicting the groundwater level (Coulibaly et al., 2001; Feng et al., 2008; Lallahem et al., 2005; Sahoo et al., 2017). In contrast, other models are designed to make predictions based on historical groundwater level data (Chang et al., 2016; Chen et al., 2010; Solgi et al., 2021; Yang et al., 2015).

Common machine learning (ML) models applied in groundwater

level prediction are Multiple Linear Regression (MLR) (Sahoo and Jha, 2013), multi-layer perception (MLP) (Müller et al., 2021; Sahu et al., 2020), gated recurrent unit (GRU) (Cai et al., 2021; Gharehbaghi et al., 2022), support vector machine (SVM) (Suryanarayana et al., 2014; Yoon et al., 2011; Yu et al., 2006), Random Forest (RF) (Wang et al., 2018; Yin et al., 2021), neural network (NN) (Coppola et al., 2003; Coulibaly et al., 2001; Feng et al., 2008; Lallahem et al., 2005), adaptive neuro-fuzzy inference system (ANFIS) (Samani et al., 2022), genetic programming (GP) (Cobaner et al., 2016; Fallah-Mehdipour et al., 2013; Kasiviswanathan et al., 2016) and others (Rajaee et al., 2019).

Furthermore, utilizing deep learning for groundwater level change modeling became appealing with many studies published recently. In particular, the recurrent neural network (RNN) and others exhibited a promising output in groundwater level prediction and modeling (Xu et al., 2019). The Deep Learning models are capable of automatically extracting complex trend variations without the need of preprocessing steps. A long short-term memory (LSTM) networks is a type of recurrent neural network (RNN) capable of processing sequential data such as timeseries, text and speech (Hochreiter and Schmidhuber, 1997). The LSTM was recently adopted by many researchers for the prediction of groundwater and was applied in many aquifers and showed high accuracy (Afzaal et al., 2019; Bowes et al., 2019; Jeong and Park, 2019; Kochhar et al., 2022; Müller et al., 2021; Sun et al., 2022; Wunsch et al., 2021b).

Several studies have used only the groundwater level data without restoring or forcing in any other meteorological data to predict the groundwater levels using LSTM (Solgi et al., 2021). Many papers assessed the LSTM and concluded that it has a superiority over other machine learning models such as Random Forest, Artificial Neural Network and simple NN (Müller et al., 2021; Solgi et al., 2021; Wunsch et al., 2021a; Yin et al., 2021). Other studies showed that Random Forest (RF) outperformed other machine learning models in reflecting the dynamic of groundwater level change (Rodriguez-Galiano et al., 2015; Youssef and Pourghasemi, 2021).

The integration of remote sensing products for the prediction of groundwater level in an aquifer with various parameters influencing its fluctuation can increase the accuracy of the prediction. Previous research integrated hydrological parameters such as (temperature, precipitation and historical groundwater level data) as an input to predict groundwater level (Rajaee et al., 2019). Other factors like the abstraction rate, and the hydraulic connection between the aquifers could impact the groundwater level, but it is challenging to monitor it regularly (Wunsch et al., 2021a). The Gravity Recovery And Climate Experiment (GRACE) satellites capture the total storage for the entire aquifer. Several studies have used GRACE in estimating the groundwater storage change regionally and locally (Alghafli et al., 2023b; Bhanja et al., 2016; Chen et al., 2019; Shamsudduha et al., 2012). GRACE could be used to improve the model prediction and estimation. Thus, coupling GRACE with the In-situ observations and other remote sensing products using LSTM and RF models will be investigated. Previous research that forced GRACE products using machine learning for the prediction of groundwater level concluded it improved the performance of the models (Liu et al., 2021; Mukherjee and Ramachandran, 2018; Sun, 2013). Limited studies coupled GRACE products with data driven models for the purpose of groundwater level prediction (Ali et al., 2022; Khorrami et al., 2023; Malakar et al., 2021; Seyoum et al., 2019; Yin et al., 2021; Zhang et al., 2020).

Recent studies have investigated the impact of El Niño-Southern Oscillation (ENSO) on the response of groundwater level change and concluded that it has a strong influence (Batista et al., 2018; Fleming and Quilty, 2006; Kolusu et al., 2019; Sulaiman et al., 2023; Susilo et al., 2013). The ENSO phenomenon is a key driver influencing global climate variability and the rainfall characteristics (Capotondi et al., 2015). The sea surface temperature of the central eastern Pacific is linked with the global rainfall variation. In literature, the El Niño and La Nina phenomenon has been evident to impact the rainfall characteristics globally. Within the data-driven approaches limited studies integrated the index of ENSO in the machine learning models (Kalu et al., 2022).

While various studies have applied machine learning techniques in groundwater (Bordbar et al., 2022), significant gap remains, especially in regions like the Arabian Peninsula, where groundwater resources are experiencing significant depletion. There is no research that has explored the integration of remote sensing products with ML techniques for groundwater level prediction in Abu Dhabi Emirate, United Arab Emirates, where groundwater faces major drawdown. Furthermore, the influence of large-scale climate drivers, such as the ENSO on the groundwater levels remains unexplored. There are no studies that assessed the impacts of ENSO on groundwater storage change in this region or incorporated the ENSO index into ML models for the groundwater level prediction. Therefore, this study aims to address these gaps by developing a regional model for predicting the monthly groundwater storage change in Abu Dhabi Emirate. Moreover, we investigate the role of the ENSO on the temporal variability of groundwater level.

The groundwater depletion in Abu Dhabi Emirate is mainly attributed to the emirate's economic development and agricultural area expansion. Over the last three decades, groundwater levels near agricultural areas have declined more than 120 m (Alsharhan and Rizk, 2020). The UAE government reduced the pressure on groundwater resources when the water domestic use shifted from groundwater to desalinated water, yet the aquifer systems in UAE continue to decline due to the ongoing agricultural practices. Effective management and sustainable planning of groundwater resources is required. To achieve that, an accurate simulation of groundwater storage change is needed. A robust model could help on understanding the different parameters influencing the groundwater storage change and seek for effective policies for the purpose of preserving the groundwater resources. Thus, the LSTM and RF models are utilized to train a model using inputs such as terrestrial water storage, soil moisture, precipitation, evapotranspiration, and the El Nino Index. The selected inputs are chosen based on previous research that have concluded these data have high influence on the groundwater storage variations (Adiat et al., 2020; Ali et al., 2024; Sahoo et al., 2017; Samani, 2024). These models will be optimized for the highest accuracy with the generation of a model that can accurately predict the groundwater levels. This assessment will help draw a conclusion on what ML models could simulate the groundwater level over the Abu Dhabi Emirate.

The aim of the present study is to develop a regional model to predict the monthly groundwater storage change within the aquifer system of Abu Dhabi emirates. This model will support decision makers on understanding the aquifer dynamics and evaluate the regional groundwater using remote sensing products solely. The sensitivity analysis is employed to explore the influence of the input parameters on the model output's performance and to understand the interaction between the input data within the developed model. To our best of knowledge, this is the first research apply the LSTM and other machine learning techniques in the United Arab of Emirates for the prediction of groundwater level coupling GRACE and other remote sensing products (Nourani et al., 2024). The extensive datasets acquired from the Environment Agency of Abu Dhabi give this research an advantage in trusting the output and will support the analysis and the validation. Furthermore, this study examines the influence of the ENSO phenomenon's on precipitation patterns and, consequently, on groundwater level fluctuations within the region. There is no research that has assessed the impact of El Nino in the groundwater over the Arabian Peninsula and limited studies incorporated El Nino in the LSTM and RF models. Overall, the development of a regional model that incorporates environmental and climatic variables is highly advantageous for formulating climate adaptation strategies under future scenarios on a national scale. We believe that our study offers valuable insights that can advance future groundwater modelling in the UAE, facilitating better-informed decision-making.

2. Study area and datasets

2.1. Study area

Abu Dhabi emirate is located in an arid climate zone with limited precipitation and the inland area of Abu Dhabi is around 80,000 km^2. The precipitation varies spatially from 90 mm/year in coastal areas to 160 mm/year on the eastern region of Abu Dhabi near the mountains (Alsharhan and Rizk, 2020). The evaporation rate is averaged 2000 mm annually. The obtained data for groundwater monitoring wells are within the Abu Dhabi Emirate (Fig. 1). The Quaternary unconfined surficial aquifer geology consists of sand, gravel, sand and gravel, and Sabkha sediments. Due to the high depletion rate near agricultural areas that is exceeding the recharge rate, the groundwater level has declined by 100 m near the agricultural areas. The groundwater resources are mainly used to meet the demand of agricultural irrigation purposes with an annual abstraction of 2.7 billion cubic meters (Sherif et al., 2021). The groundwater is also used for oil production and recovery, but no data are available on these wells abstraction rate. A cone of depression exists near the agricultural areas where the majority of farms increased the wells depth reaching the limestone aquifer. To align with the aim of this study, both the quaternary and limestone aquifers' data are used in the analysis to further understand the groundwater storage change regionally. Additionally, GRACE signal captures terrestrial water storage in all depths; thus, it cannot distinguish between the two aquifers. The signal from GRACE could also be influenced from the abstraction of groundwater from the limestone. As a result, both aquifers are considered in the analysis.

2.2. In-situ groundwater

A groundwater monitoring network was established for the assessment of the groundwater resources over Abu Dhabi Emirate. The daily groundwater level data is obtained from the Environment Agency of Abu Dhabi (EAD) for the 263 monitoring wells (Fig. 1). The majority of the monitoring wells represent the shallow unconfined aquifer whereas several wells are deployed with dual telemetric devices representing the shallow unconfined aquifer, the limestone aquifer and Sabkha aquifer. Prior to using the groundwater level data, the data with outliers were removed from the calculation. For example, if the trend shows a sudden jump with no heavy rainfall events occurs before, these records are removed. The obtained groundwater data period is from 2003 to June-2023 in a daily time step. Certain wells show a gap for months or years due to the battery issues with the telemetric devices; therefore, these gaps were not interpolated. Missing data could cause a problem by reducing the statistical power of the data and this could result in bias (Kang, 2013). Instead, when averaging the groundwater level data, the weight of these wells is not considered in these dates. All the data is measured using telemetric devices and none are taken manually. The groundwater timeseries for the monitoring wells show a different timespan because of the difference in the commissioning and decommissioning of the wells. Thus, averaging the data with no interpolation applied will reduce the uncertainties associated with the interpolation techniques. The monthly time steps are considered for the analysis to ensure a match in the temporal resolution between the groundwater level data and the remote sensing products.

2.3. Selected predictors

Five variables were selected as groundwater level predictors. These variables are Terrestrial Water Storage Anomalies (TWSA), soil moisture, precipitation, evapotranspiration, and ENSO. These variables directly influence groundwater resources, thereby providing insight into fluctuations in groundwater levels. Precipitation acts as a primary driver of groundwater availability and recharge, while evapotranspiration reflects climatic and land use characteristics (Sherif et al., 2018). Additionally, soil moisture serves as an indicator of irrigation practices and potential irrigation return flow. TWSA information from GRACE data, when integrated with unsaturated zone information (i.e., soil moisture), can aid in interpreting observed changes within the saturated zone (Alghafli et al., 2023b). Most importantly, ENSO is known to have a strong impact on the precipitation in the region (Niranjan Kumar and

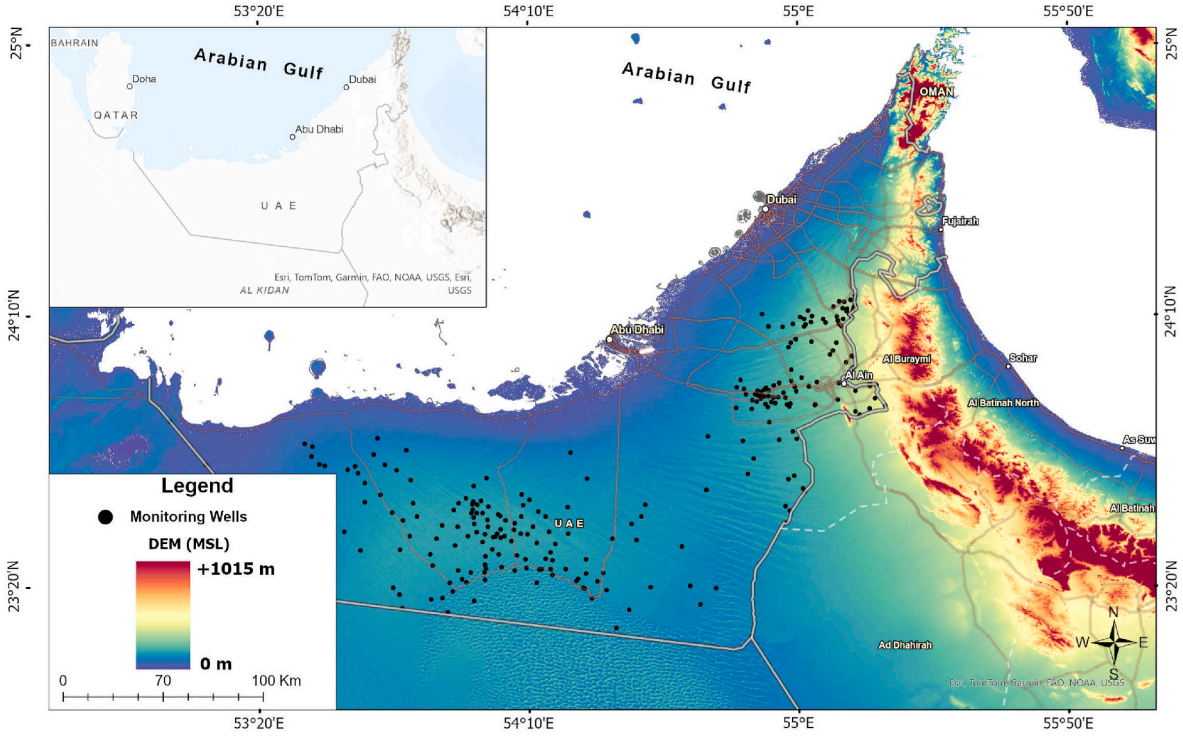

Fig. 1. The geographical location of the study area and groundwater monitoring wells obtained from the Environment Agency of Abu Dhabi.

Ouarda, 2014).

2.3.1. Terrestrial water storage

GRACE products capture the monthly terrestrial water storage in the globe and come in two forms namely spherical harmonic (SH) and mass concentration (mascon) (Tapley et al., 2004). The main difference between the two forms is in the preprocessing steps and the models integrated for the corrections (Swenson and Wahr, 2006). These solutions are processed by different centers, and each has its own unique approach. In this research, Release 6 (RL06) is used obtained from three SH solutions (known also as GSM) and two mascon solutions. The terrestrial water storage is processed by three GRACE centers which are the Center for Space Research (CSR), NASA JET Propulsion Laboratory (JPL), and GeoforschungsZentrum Potsdam (GFZ). Even though GRACE products come in a resolution of 0.25°, 0.5° and 1°, the native resolution of GRACE is 3° × 3° (Tapley et al., 2004). The mascon solutions used in this study is processed by JPL and CSR. Due to battery issues, GRACE was decommissioned on 2017 and GRACE FO altered the previous satellite starting from 2018. The two years gap was ignored in the analysis for the purpose of reducing the uncertainty and errors.

2.3.2. Soil moisture

Multiple soil moisture products were derived and input in the model for the purpose of predicting groundwater level. The Global Land Data Assimilation System (GLDAS) simulates the energy and water cycle fluxes in monthly scale by forcing observation and satellite data in a land surface models (Rodell et al., 2004). The soil moisture fluxes were obtained from GLDAS version 2.1 for the analysis. In this study, the soil moistures products are obtained from GLDAS models namely the GLDAS catchment land surface models (CLSM) (Li et al., 2018, 2019), Noah model (Beaudoing and Rodell, 2020a) and Variable Infiltration Capacity (VIC) model (Beaudoing and Rodell, 2020c; Hamman et al., 2018). These models are different in their structures, parameterization, and validation process to estimate the soil moisture flux. The time resolution for the products was aggregated to a monthly average.

Noah model features a multi-layer soil moisture model product with a capability of integrating the interaction between soil vegetation and atmosphere (Beaudoing and Rodell, 2020b). The penetration depth of Noah is up to 2 m. A layer from 0 cm to 200 cm was used in the analysis. The VIC model applies a unique approach to simulate the soil moisture by integrating the soil's characteristics and soil's water capacity storage (Hamman et al., 2018). VIC is used for regional scale areas and has a coarse resolution. All the soil moisture data were averaged.

2.3.3. Precipitation

Based on previous research, the following precipitation products showed good agreement with In-Situ precipitation gauges over UAE. The Climate Hazard Group InfraRed Precipitation with Station data version 2.0 (CHIRPSv2) (Funk et al., 2015) and the PERSIAN Climate Data Record (CDR) products (Sorooshian et al., 2014) are used in this study. Previous research concluded that both products outperformed other rainfall products over the UAE (Baig et al., 2022). Thus, both are used in the analysis. CHIRPSv2 is generated based on 14,000 gauges with monthly records and 200,000 gauges with daily records. It also uses CFSR reanalysis datasets when gaps exist in the data. It integrates the TRMM 3B42 precipitation products during the data generation process. The spatial resolution of CHIRPS is 0.05° with a time range spanning from 1981 to present. PERSIAN CDR have multiple input data for the precipitation generation and incorporate observation data obtained from the Climate Prediction Center (CPC) and the National Center for Environmental Prediction for the calibration process (Sadeghi et al., 2021). The precipitation data are bias corrected using the data from the Global Climatology Project (GPCP) V2.3 (Sadeghi et al., 2019). The acquired precipitation data from PERSIAN CDR provides a daily precipitation estimates in a 0.25° × 0.25° spatial resolution from 1983 to present. All data were aggerated to obtain monthly scale precipitation to match with the other datasets for the groundwater level prediction.

2.3.4. Evapotranspiration

The Global Land Evaporation Amsterdam Model (GLEAM) simulates evapotranspiration (ET) by including the transpiration, bare soil evaporation, open water evaporation, interception loss, and snow sublimation. ET plays a key role in the hydrological cycle and could have an impact on the climate through feedback mechanisms (Shen et al., 2015; Shukla and Mintz, 1982). Two dataset versions available from GLEAM and the main difference between both are the forcing datasets during the process of estimating ET. GLEAM v3.7a is forced by satellite and reanalysis data whereases the GLEAM v3.7b is forced solely by satellites datasets (Martens et al., 2017; Miralles et al., 2011).

GLEAM has been validated globally and outperformed other ET products (Alghafli et al., 2023a; Ding and Zhu, 2022; Wang et al., 2022; Yang et al., 2017). There is no study that compared different ET datasets over the study area nor validated GLEAM over the study area. Since GLEAM showed better agreement in other regions, it was used as an input for the groundwater level model. The ET derived from GLEAM is in a 500-m resolution spanning from 1980 to 2022 for the GLEAM v3.7a and from 2003 to 2023 for GLEAM v3.7b. To match with the time range of the other datasets, GLEAM v3.7b was used in this study area and the daily scale was aggregated to monthly scale to ensure a similar temporal resolution with the other datasets.

2.3.5. El Niño southern oscillation (ENSO)

The influence of the Pacific Ocean temperature results in a global climatic response. The temperature and wind interchange causes a famous El Nino event during warm ocean water and La Nina event occurs when the Pacific Ocean sea surface temperature is colder than the averaged sea surface temperatures (Ropelewski and Halpert, 1986). A common metric used to characterize the El Nino phenomenon is called the El Nino 3.4 index which is an anomaly representing the sea surface temperature in a location located in the central equatorial Pacific Ocean spanning from 5° N to 5° S latitude and from 170° W to 120° West longitude (Trenberth, 1997). El Nino occurs if the sea surface temperature anomalies in the Nino 3.4 region is higher than 0.4 (Celsius) C° averaged over five months for at least 6 consecutive months (Trenberth, 1997). The Pacific sea surface temperature (SST) was analyzed with respect to the rainfall globally and it was concluded that the SST anomaly is linked with the rainfall variations (AlEbri et al., 2016; Diro et al., 2011; Gleixner et al., 2017; Thielen et al., 2023). In the Arabian Peninsula, several studies investigated the relationship between rainfall and El Nino (Abid et al., 2016; AlEbri et al., 2016; Atif et al., 2020; Horan et al., 2023; Niranjan Kumar and Ouarda, 2014). In the context of groundwater, there is no study that evaluated the influence of El Nino phenomenon in the groundwater level fluctuation in the Arabian Peninsula. Even though the relation is indirect through the rainfall and eventually through the groundwater recharge from rainfall, its input in the model will help in finding a relation between this phenomenon and the groundwater recharge. El Nino 3.4 index was obtained for the purpose of understanding its impact on the groundwater level (Rayner et al., 2003). The statistical values of the input data are described in detail in supplementary material (Table S.1) for the training and testing datasets.

2.4. Data scaling

Data are averaged for each hydrological parameter leaving one record for TWSA, soil moisture, and precipitation. The utilized data for the analysis shows variation and difference in the magnitude, which hinders the applied model ability to learn for the prediction of groundwater level. A common approach to keep the input data consistent in the scale and ensure its convergence, is to scale the data. In other words, input parameters with a large variation in scales could lead the model to favor the parameters that have a large range and ignore those with a smaller range. Thus, the input data were scaled using the min-max normaliza-

tion technique prior to the model development (Eq. (1)). The MinMaxScaler from the scikit-learn python packages was employed to rescale all the input parameters (Pedregosa et al., 2011). This normalization approach has been successfully applied in hydrological studies that focused on developing a ML model (Jeong and Park, 2019; Patra et al., 2023; Yaseen et al., 2016)

$$X_{(ij)scaled} = \frac{(X - X_{min})}{(X_{\max - X_{\min}})} \quad (1)$$

Where X_{scaled} represents the scaled data in a ith month and jth year, X is the data in ith month and jth year. X_{min} is the X minimum and X_{max} is the X maximum.

The spatial averaging of environmental variables inherently overlooks spatial variability. Nevertheless, we consider this approach adequate for our objective of investigating the temporal variability in environmental variables and its relationship with groundwater level fluctuations. It is important to acknowledge that localized interactions may exhibit distinct behaviors, which lie beyond the scope of this study.

3. Methodology

In this study, the LSTM and RF models are developed for groundwater level prediction. These models were chosen due to their widespread application in groundwater level forecasting. The LSTM model is particularly advantageous because it retains memory of historical events, which is crucial for groundwater studies (Tao et al., 2022). Meanwhile, RF offers a straightforward and less computationally intensive algorithm that is both reliable and commonly used in groundwater level predictions (Afrifa et al., 2022). Moreover, the impact of lags on the accuracy of the deep learning models have been investigated. Its influence should be considered where it could enhance models. The lags up to −6 months lag were considered on all the datasets. All the datasets are normalized following the suggestion of Lawrence et al. (1997). The datasets are split into two periods. From 2002 to 2019 for training and 2020 to 2023 for the validation. Thus, the training and testing splits are 85% and 15%, respectively. The input parameters are assessed using statistical analysis to understand the relationship between the variables.

A common approach to analyze the relationship between the variables and to choose the important variables for the model is to use correlation coefficient (Derbela and Nouiri, 2020; Vu et al., 2021). However, having a strong correlated predictors could negatively impact the performance of the developed model due to the effect of the collinearity (Bouramtane et al., 2023). Therefore, the importance of the variables used in the study is assessed by conducting a sensitivity analysis, which investigates how the variations in the predictors can impact the variations in the model response (groundwater level in our case). In this study, the Global sensitivity analysis and the feature importance method are applied. Feature importance is a strength of Random Forest (unlike LSTM), as it quantifies the significance of predictors based on their contribution to the target variable (i.e., groundwater level). This is determined by calculating the increase in error when a predictor is removed, with higher errors indicating greater predictor importance. For regression problems, the error is represented

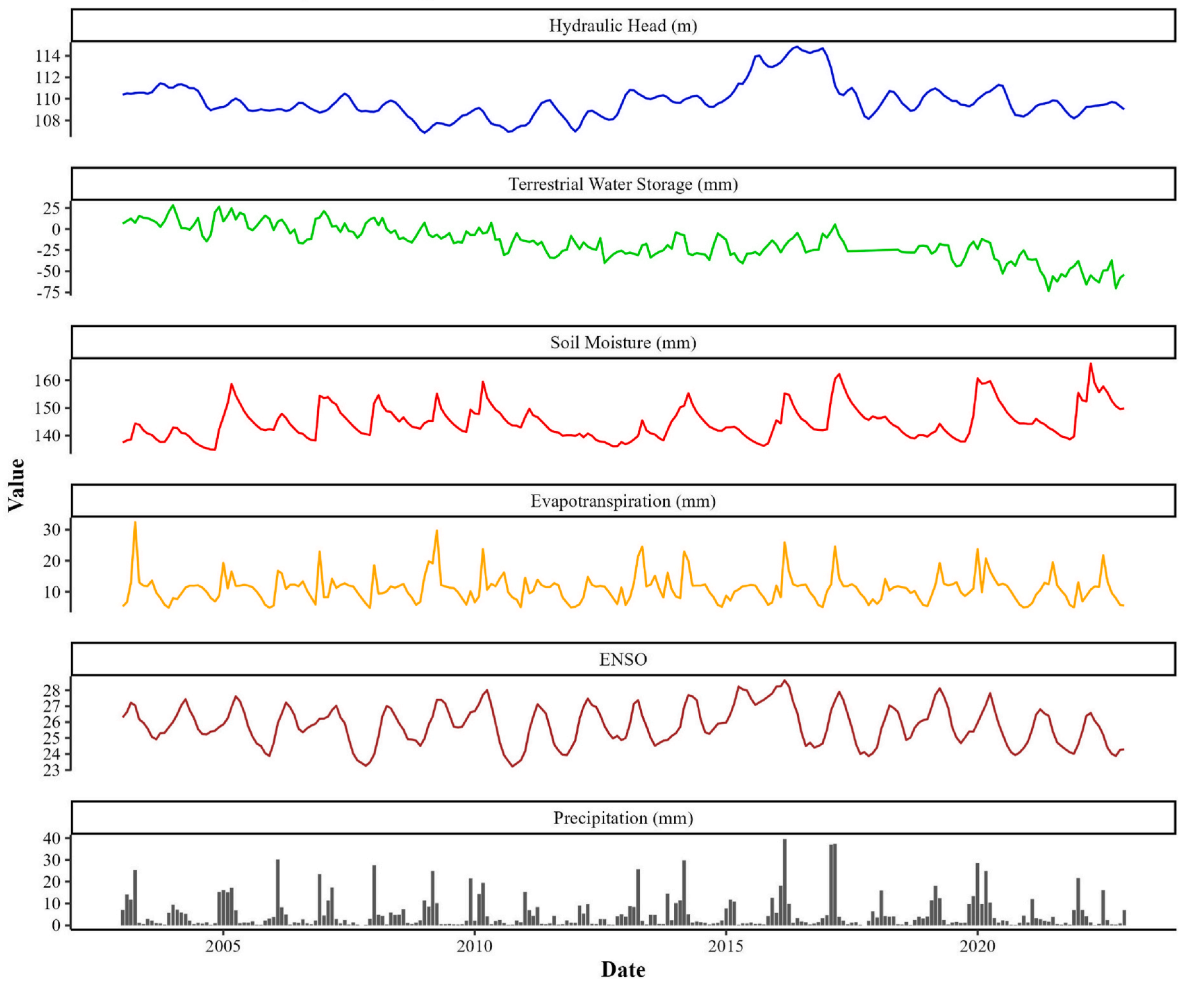

Fig. 2. The input parameters used for developing LSTM and RF models.

by the mean square error. Since the LSTM model does not inherently provide feature importance, we further conducted sensitivity analysis. Both methods help interpreting the most important variables in the machine learning model and which variable is more sensitive to the machine learning model. Sensitivity analysis will highlight the significance of each variable. The input data for developing the models are displayed in Fig. 2. The methodology flowchart for this study is illustrated in Fig. 3.

3.1. Long short-term memory neural network (LSTM-NN)

LSTM is part of the recurrent neural network (RNN) family (Hochreiter and Schmidhuber, 1997; Rumelhart et al., 1986). It is commonly used for time series and sequence data modeling. The LSTM learning process is distinguished from the known RNN since it is not restricted only to backpropagation but forward propagation as well from the previous data. LSTM does not suffer from vanishing gradient problems since it is mainly designed to memorize long term dependencies in sequential data (Hochreiter and Schmidhuber, 1997). On the other hand, RNN models usually suffer with the vanishing gradients when the sequence gets longer resulting in the disconnection of information across a long distance in the sequence. The memory cell in LSTM manages multiple data with several gates (input, output, and forget gate) to control the needed and ignored information (Hochreiter and Schmidhuber, 1997). The gates regulate the information whether to eliminate or add the information to the cell state. In other words, LSTM has a complex network structure with three gates to control the flow of information. Each gate has a sigmoid neural net layer and its value ranges from 0 to 1 indicating how much of each component should be accepted. For example, a value of one indicates that all the information will go through while a value of zero means nothing will go through. The forget gate determines the needed information and whether it should be ignored or kept (Gers et al., 2000). It decides if this information is relevant or not. The input gates update the cell with the chosen values to update the cell memory. A hyperbolic tangent function is applied to rescale the information between [−1,1]. If the calculated value from the input gate is negative, the information will be subtracted from the cell state, whereas a positive value will indicate an addition. Finally, the output gates decide the needed elements of the cell memory to update the hidden state of the cell. The cell memory helps the LSTM on controlling the long term dependencies since the information could remain in the memory for multiple steps (Hochreiter and Schmidhuber, 1997).

The architecture of the LSTM consists of four key elements: the Constant Error Carrousel cell and three gates: input gate, output gate, and forget gate as depicted in Fig. 4. The information is processed through a series of sequential calculations executed iteratively. The following equations are used for developing the LSTM model and specifically for the calculation of the hidden vector h_t for the LSTM model:

$$f_t = \sigma\left(w_f\, h_{t-1} + U_f\, x_t + b_f\right) \quad (2)$$

$$i_t = \sigma\left(w_i\, h_{t-1} + U_i\, x_t + b_i\right) \quad (3)$$

$$o_t = \sigma\left(w_o\, h_{t-1} + U_o\, x_t + b_o\right) \quad (4)$$

$$C'(t) = \mathrm{Tanh}\left(w_c\, h_{t-1} + U_c\, x_t + b_c\right) \quad (5)$$

$$C_t = f_t \otimes C_{t-1} + i_t \otimes C_t \quad (6)$$

$$h_t = o_t \otimes \mathrm{Tanh}(C_t) \quad (7)$$

Where i_t, f_t, o_t, and $C'(t)$ are the values of the input, forget, output gates and the memory cell in the memory block. C_t is the memory cell state at time t. The h_t is the initial state at time t while the h_{t-1} is the previous hidden state of the cell at time t-1. b_i, b_f, b_o and b_c are the bias terms for the input, forget, output gates and new information respectively. The w_i, w_f, w_o and wc represent the weights for each gate. The U_f, U_i, U_o and U_c are the weights associated with the gates for input xt at time t. The σ represents the sigmoid activation function. The tanh is the hyperbolic tangent function to regulate the values flowing through the network. The LSTM model was developed in Python 3.9 using the Keras packages with TensorFlow backend (Joseph et al., 2021).

During the configuration process, the overfitting was carefully considered. The overfitting could result in a perfect model during the training only where outliers could influence the model resulting in poor prediction outcomes. During training, multiple time steps are used in the calculation to look back and provide the best overall models. The following timesteps are used to choose the most optimum models (3, 6, 8, 10,12 months).

3.2. Adam optimizer

Optimization algorithms are used to minimize the loss function during the model training. A common optimizer algorithm used are Adam and Root Mean Square Propagation (RMSprop) where these algorithms help on the reduction of errors when applying LSTM algorithm. Adam optimizer tis a Stochastic Gradient Descent algorithm used for

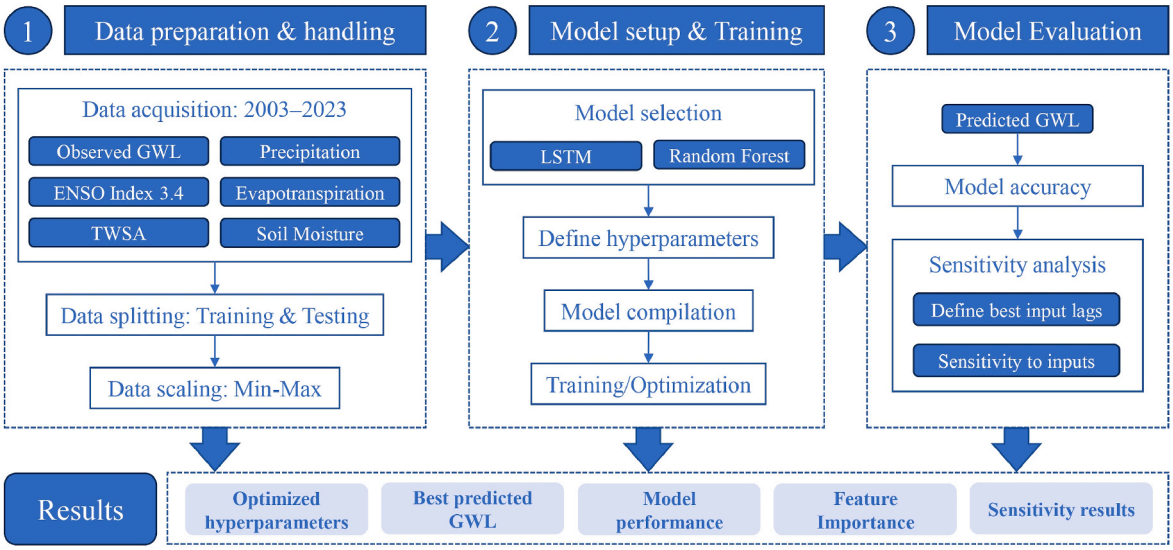

Fig. 3. Pseudocode illustrating the groundwater level prediction process, incorporating all input variables.

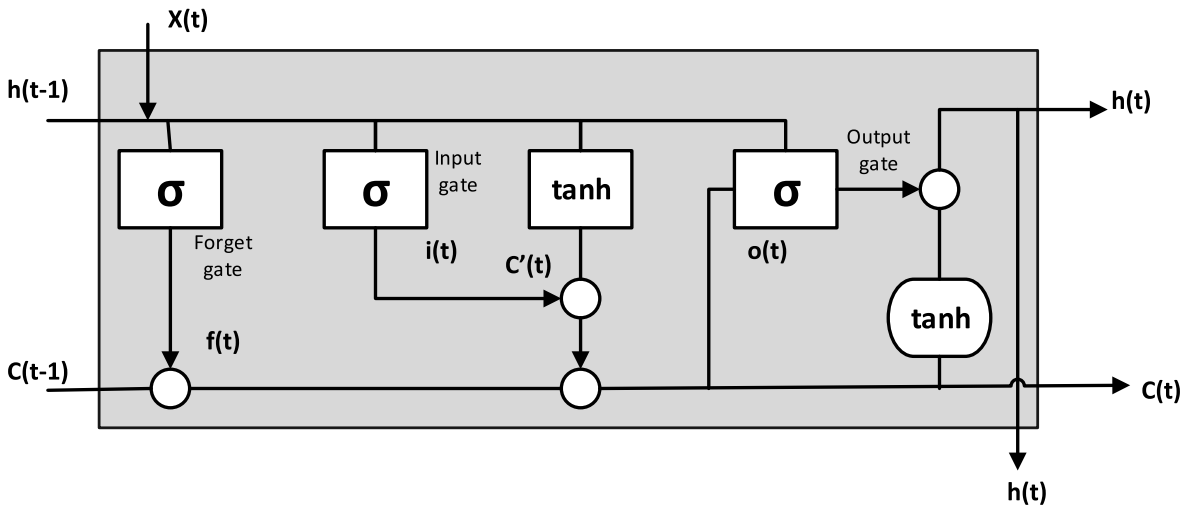

Fig. 4. LSTM module with the layers.

discrete optimization combining the RMSprop (Tieleman and Hinton, 2012) and Adaptive gradient (AdaGrad) algorithms (Duchi et al., 2011; Kingma and Ba, 2014). It converges faster and resulted in a better performance than the stochastic gradient descent (SGD) (Kingma and Ba, 2014). The LSTM with ADAM optimizer trained using the mean square error (MSE) as the loss function. The initial learning rate that was applied for the developed LSTM model is 0.001.

3.3. Random forest

Random Forest (RF) regression is an ensemble learning approach that could be used for classification and regression tasks. The RF belongs to the family of decision tree employs multiple trees to define the best trees with the highest correlation (Breiman, 2001). RF regression develops multiple decision trees during training and the output in the case of regression task is the average prediction. RF is capable of handling non-linear relationships between variables for the purpose of predicting groundwater level. Each tree is built from a different random sample of the data and the replacement is done using bootstrapping resampling technique. The final prediction of the RF model is the average of all the individual decision tree predictions. Using multiple trees helps reduce a common issue with individual decision trees which is the risk of overfitting.

RF performance depends on the hyperparameters such as number of trees, sample size, minimal node size and the number of input parameters for the splitting of each node (Biau and Scornet, 2016). RF models consist of multiple decision trees, each contains a series of nodes that also branch off into additional nodes by splitting the data based on the given criteria and finally it reaches a terminal node. A terminal node is when additional splitting is not required (i.e., meeting the predefined criteria) or may not be possible. The data was split into training and testing periods. The training period is from 2003 to 2019 while the testing period is from 2020 to 2023.

3.4. Model evaluation criteria

Multiple statistical metrics are used to assess the accuracy of the developed groundwater level model during the training and validation phases; the Nash-Sutcliffe model efficiency (NSE) coefficient (Eq. (8)), the coefficient of determination (R^2; Eq. (9)), the Root Mean Squared Errors (RMSE; Eq. (10)) and the Percent Bias (PBIAS; Eq. (11)). These errors and linear fitting metrics are applied to test models' performance and have been widely used (Ali et al., 2023; Sarkar et al., 2024). The optimum groundwater level model will yield an NSE and R^2 equal to one and RMSE and PBIAS equal to zero.

$$NSE = 1 - \frac{\sum_{i=1}^{n}(G_i - S_i)^2}{\sum_{i=1}^{n}(G_i - G_{mean})^2} \tag{8}$$

$$R^2 = 1 - \frac{SS_{res}}{SS_{tot}} \tag{9}$$

$$RMSE\ (mm) = \sqrt{\frac{1}{n}\sum_{i=1}^{n}(S_i - G_i)^2} \tag{10}$$

$$PBIAS = \frac{\sum_{i=1}^{n}(G_i - S_i)}{\sum_{i=1}^{n}(G_i)} \times 100 \tag{11}$$

where G_i is the observed monthly groundwater level from the telemetric monitoring wells at time i, S_i is the predicted groundwater level derived from LSTM or RF models. G_{mean} is the mean of the monthly groundwater level. SS_{res} is the sum of residual squared and SS_{tot} is the total sum of squares.

3.5. Sensitivity analysis methods

The feature important method is utilized for the RF model to analyze the effect of input variables on the model's output, while the global sensitivity analysis is applied for both RF and LSTM models. The global method assess the impact of the uncertain input by varying the parameters simultaneously (Song et al., 2015). This approach incorporates the impact of the input variables over the whole range of variation, making it proper for non-linear models. This method has been widely used in the field of hydrology (Baroni et al., 2018; Baroni and Tarantola, 2014; Makler-Pick et al., 2011; Rosolem et al., 2012).

There are various methods within the global sensitivity framework, this study employs the Sobol method (Sobol', 1990; Sobol', 1993) for both LSTM and RF models. The Sobol method applies variance decomposition to assess the contribution of each uncertain input variable to the overall output variance of the model. The first-order and total-order Sobol's indices are utilized to examine the total contribution of each parameter to the output variance and assess the individual effects as opposed to its interaction with other parameters.

In other words, the Sobol method is a variance based global sensitivity analysis approach that can assess the influence of each input variable on the groundwater level model performance and the total-

order Sobol' indices determine the interaction between these variables within the groundwater level model (Zhang et al., 2019). This method will give an insight on understanding the variables and which variables has the highest impact on groundwater storage change.

4. Results

This section presents a comprehensive analysis and comparison of the developed models through statistical analysis. Then, a comparison between the LSTM and RF is conducted using statistical metrics. The 95% confidence bound is used to measure the uncertainty associated with each model. An optimization technique is utilized to demonstrate the importance of the lags in improving the developed models. Finally, a sensitivity analysis is applied to identify the impact of each variable on model performance.

4.1. Hyperparameters results for LSTM and random forest

The hyperparameters achieved the highest performance for the LSTM and RF are shown in Table 1. These hyperparameters are carefully chosen and tuned, while the learning rate is adjusted for the parameters based on the ADAM optimization algorithm. The drop out is used to avoid the overfitting of the model and serves as a robust regularization technique (Hinton et al., 2012). Furthermore, having too many neurons is time consuming where significant computational demand is required. The high number of neurons could also lead to an overfitting whereas a small number of neurons could weaken the network's learning ability (Zhang et al., 2018). Therefore, the chosen neuron number in this study for the optimal model is 20 hidden neurons (Table 1). The batch size indicates how many data points are processed to update the model weight.

4.2. Model performance assessment

Four statistical metrics are used for the assessment of the LSTM and RF models during the training and testing periods. The statistical metrics results for the two models are summarized in Table 2. The RF model outperformed the LSTM model during the training, while LSTM slightly outperformed RF during the testing. Both models were able to capture the seasonal fluctuations for the groundwater level during the training and testing periods (Fig. 5). Data with lags up to 6 months are incorporated in the analysis. Best models performance were achieved when using lag −3 months for LSTM and −6 month for RF model. Thus, based on both periods, the RF model has better accuracy than the LSTM model. Overall, both models showed acceptable results.

It is clearly shown that the significant rise in groundwater level in 2016, due to the heavy rainfall storms, is captured by the model (Fig. 5). Previous studies have indicated that the El Nino years brings an exceptional precipitation rates above the average in the UAE (AlEbri et al., 2016). Specifically, 2016 was an El Nino year where precipitation amount was higher than the average contributing to recharge the aquifers in Abu Dhabi Emirate. This indicates that the developed model represents a complex dynamic of the aquifer and detects the trend that exhibited the non-stationary. Between 2009 and 2011, LSTM has a higher overestimation compared to RF. Moreover, during the period 2015–2018, LSTM was less fluctuated, while RF seems to be responsive to the different signals in the input variables which may explain the better training performance.

Table 1
Hyperparameters for the optimized LSTM model.

Model	Parameter	Range	Optimized value
LSTM	Dropout rate		0.005
	Batch size		20
	Hidden Size		1
	Neuron numbers		20
	Epochs		2600
RF	Maximum depth		20
	Number of trees		20
	Minimum sample no.		2
	Maximum feature		0.8

The 95% confidence bound is applied to assess whether the models are within the 95% confidence bound or not (Fig. 6). The 95% confidence interval has been applied in previous research to assess the uncertainty associated with a model (Ballio and Guadagnini, 2004; Cooley, 1997). It is clearly shown that both models fall within the 95% confidence bounds therefore, making it inconclusive to judge which model is superior based only on this criterion. The testing period is crucial to decide which model yields better results. During the testing phase, the LSTM model yielded higher accuracy in the prediction of groundwater level. Previous research has concluded that the LSTM model has better results than the RF in predicting the groundwater level (Müller et al., 2021; Wunsch et al., 2021a; Yin et al., 2021). This finding aligns with our research, confirming that the LSTM model has better performance than other machine learning models.

4.3. Optimization for the lags effects

To examine the impact of time lags on model performance, we run LSTM and RF using the input variables with different lag times. The statistical analysis showed a significant improvement in model accuracy due to the time lags, which is attributed to the aquifer's delayed response to recharge after rainfall events. Groundwater recharge occurs when the rainfall water, irrigation return flows, or surface water bodies reach the groundwater table (Healy, 2010; Scanlon et al., 2006). The recharge occurrence varies spatially and temporally depending on various factors such as the rainfall amount, temperature, soil properties, land use and land cover change, and depth to water table (Scanlon et al., 2006).

Based on the lag analysis as illustrated in Figs. 7–9, one can see how the NSE and RMSE output improves with the lags whereas the PBIAS for both models were within an acceptable range. These plots helped on the assessment of the models in an effective way. The analysis of lags significantly enhanced both the LSTM and RF models, with improvements of 54%, 53%, and 63% in NSE, R^2, and RMSE for the LSTM model, and 59%, 63%, and 75% in the same metrics for the RF model, respectively. This highlights the crucial role of lag analysis in boosting the performance of the models.

Both LSTM and RF models successfully captured the seasonal fluctuations in the groundwater level change; thus, both models are statistically acceptable. The PBIAS optimal solution is 0 and the results from this study for LSTM and RF fall within the range of −0.1%–0.2%. A negative value indicates overestimation while a positive value indicates underestimation. Both models are close to the optimal solution; therefore, the models are acceptable. All the statistical metrics for the training and testing periods were comprehensively represented through boxplots to ease the assessment of the models (Fig. 9).

4.4. Sensitivity analysis

All the variables showed varying correlation indicating the complexity of the hydrological characteristics of the region. Based on the feature importance method applied for the RF model, it showed that ENSO index, with a six-month lag, had the most significant influence on the model, while precipitation with a two-month lag was the second most influential factor (Fig. 10). This result highlights an important aspect of the ENSO index indicating its delayed impact on rainfall pattern in UAE. This lag is due to ENSO's distant location, where it occurs near the Pacific Ocean and resulting in the delayed effect on the UAE's climate.

Precipitation is the primary source of groundwater recharge, so it significantly influences groundwater storage change. The two-month lag

Table 2
The groundwater level models evaluation during the training and testing periods.

Model	RMSE (m)		NSE		R^2	
	Training	Testing	Training	Testing	Training	Testing
LSTM	1.1	0.38	0.65	0.79	0.65	0.79
Random Forest	0.72	0.45	0.83	0.72	0.88	0.75

Fig. 5. Performance of the simulated groundwater level hydrograph over the entire modeled period. Predictions are based on two algorithms: (a) LSTM and (b) RF. The total period is divided into training (pre-2020) and testing (post-2020).

in precipitation validates an important point of groundwater recharge and the aquifer's response to precipitation. Based on the feature importance method, as displayed in Fig. 10, one can see that ENSO (−6, −5, −4), precipitation (0, −2, −3, −4), and soil moisture (0, −1) account for over 50% on effecting the RF model performance. Soil moisture also exhibited a high feature important score, indicating its impact on the RF model.

Soil moisture represents the water content in the soil influenced by rainfall, temperature, soil characteristics and all other sources of water such as irrigation water. Previous research has demonstrated the potential use of soil moisture data to predict the groundwater level and to estimate the groundwater recharge (Berthelin et al., 2023; Mathias et al., 2017). As displayed in Fig. 10, the soil moisture shows a connection with the groundwater level change, indicating its influence on the groundwater recharge. It also implies that the soil characteristics in the study area has a high infiltration rate where groundwater recharge rate is high (Sherif et al., 2018). It is worth mentioning that the majority of the landscape and forests in the study area are irrigated with treated sewage water and desalinated water (Sherif et al., 2021). Therefore, it is expected that soil moisture parameter will have an impact on the groundwater recharge.

Based on the First-order and Total order Sodol' Indices as displayed in Fig. 11a, it is clearly shown that the precipitation and the ENSO Index also have the most significant impact on the groundwater level model developed by RF. Both the feature importance method and the Sobol's method showed similar outcomes and highlighted the importance of ENSO and precipitation on the RF model. Precipitation is a major variable, influencing the groundwater change by recharging the aquifer. Previous research has concluded that precipitation plays an important role in the ML models (Lam et al., 2021a; Moravej et al., 2020). In arid regions, where surface water is scarce, precipitation is the primary source of recharge; therefore, the interaction between surface water and groundwater is absent. During rainfall events, surface water flows from the mountains through channels (Wadi) towards the desert, but these surface water only persist for days. The ENSO 3.4 Index indirectly impacts the groundwater by changing the climate pattern globally. The 95% confidence interval in the Sobol' sensitivity analysis helps to understand the uncertainty of these indices and have a robustness information about the sensitivity analysis.

The Sobol global sensitivity analysis was also applied for the LSTM model. Based on Fig. 11b, the outcomes for both the first-order and total-order Sobol Indices showed that the ENSO -3 and soil moisture −1 have the most significant impact on the LSTM model performance. Here, both the LSTM and RF models agree that the ENSO is an important parameter that influences groundwater storage change. However, the precipitation in LSTM model has the least influence which contradicts with the RF model. This could be due to the difference in models' architectures where each model has its own interpretation for the input features.

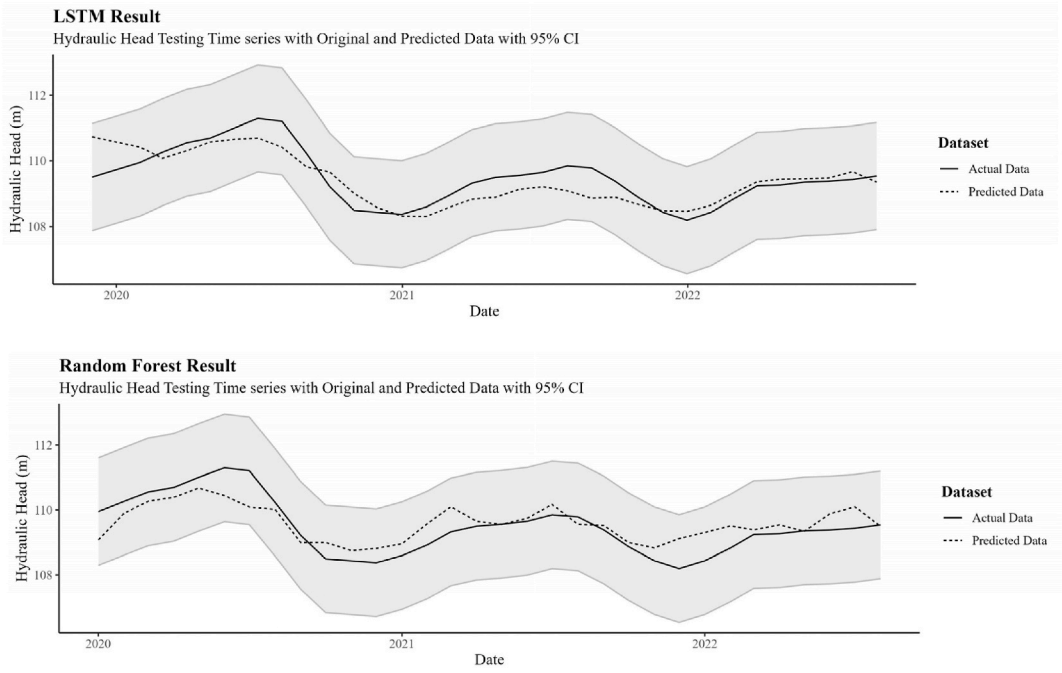

Fig. 6. Zoomed-in view of the simulated groundwater level hydrograph during the testing period (post-2020), with predictions generated using two algorithms: (a) LSTM and (b) RF. The 95% confidence bound, based on observed data calculated as 1.96*SD for, provides a measure of accuracy relative to the observed variability.

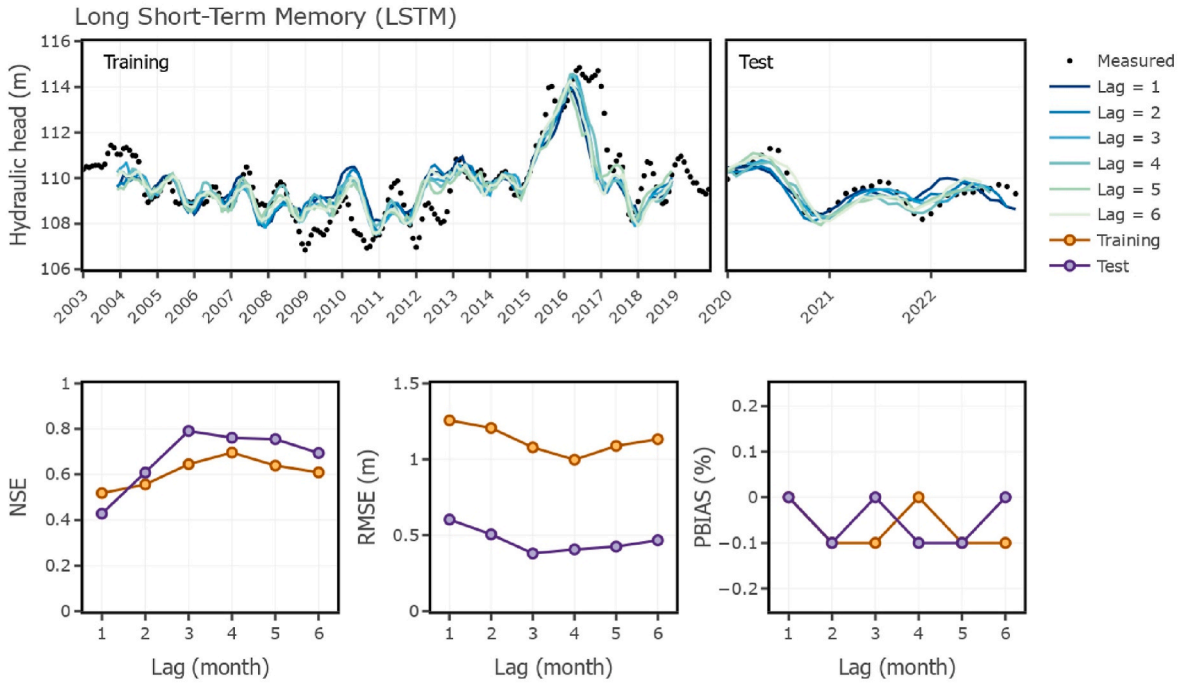

Fig. 7. The performance of the LSTM model with different lags times during the training and testing periods.

5. Discussion

5.1. Machine learning and sensitivity analysis for groundwater insights

Using 20 years of measured groundwater level at 263 locations across Abu Dhabi emirate, our study aimed to develop the models representing groundwater level changes and understand the different parameters impacting its variation. Our findings aligned with previous research that showed that LSTM outperformed RF models in groundwater level prediction (Wunsch et al., 2021a; Yin et al., 2021). This is because of the unique method adopted by LSTM where feedforward and backforward propagation are incorporated, thereby better capturing time-dependent phenomena. Although more advanced techniques are available, we selected RF and LSTM as two distinct approaches that have demonstrated their adaptability to sparse data (El-Azhari et al., 2024; Zhang et al., 2018) and their successful applications in groundwater level prediction (Feng et al., 2024; Tao et al., 2022). Moreover, previous studies have established a strong association

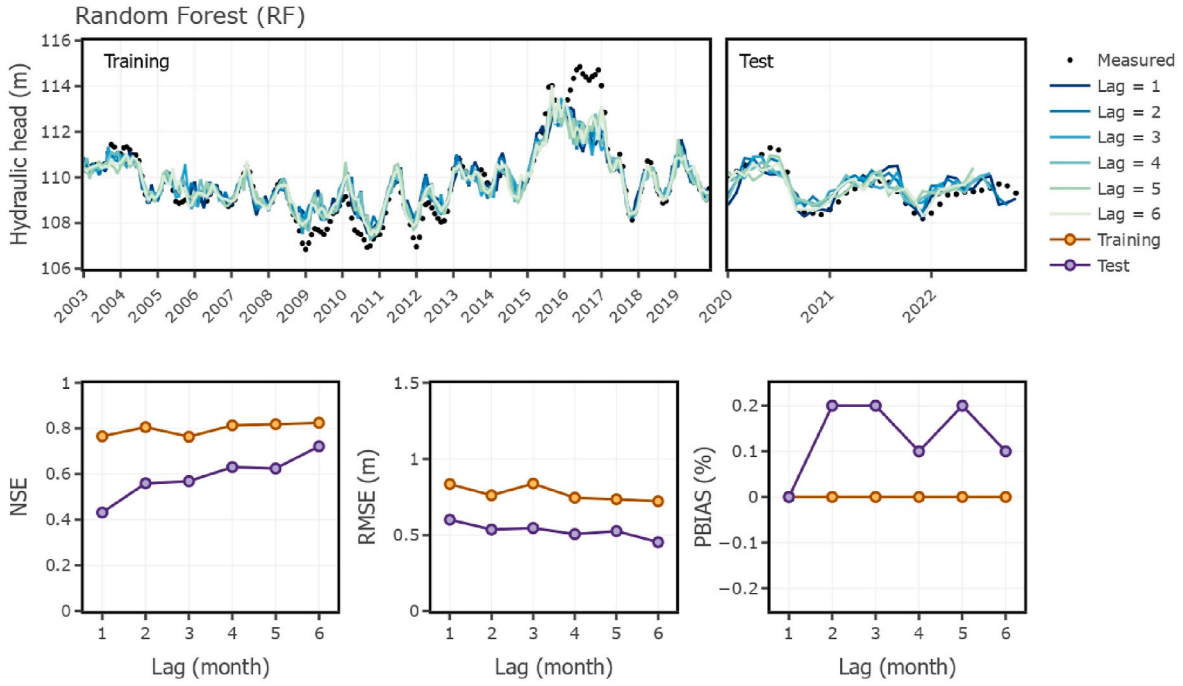

Fig. 8. The assessment of the random forest models with the lags times during the training and testing periods.

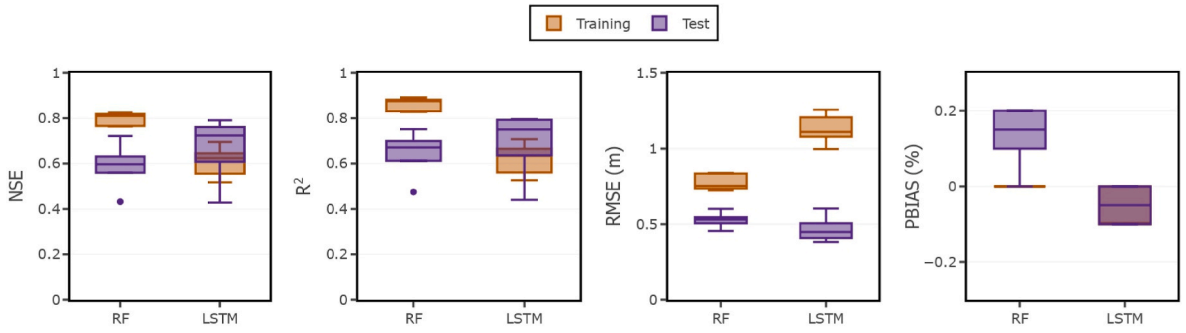

Fig. 9. A statistical metric shown in a boxplot, with whiskers indicating the 5th and 95th percentiles, to visualize model performance across different lag times.

between groundwater level and El Niño, highlighting its significant influence on groundwater variability (Batista et al., 2018; Fleming and Quilty, 2006; Hund et al., 2021; Kolusu et al., 2019; Susilo et al., 2013). Thus, this index is an important factor to consider for groundwater studies and to understand the groundwater recharge dynamic. In our research, the model considered multiple parameters and showed an acceptable result to rely on for monitoring the groundwater resources across the Emirate regionally.

Although ML models are black box models which could be a disadvantage when compared to numerical models, applying sensitivity analysis can give an insight into the parameters and how they interact with each other (Borgonovo et al., 2017; Ratto et al., 2007). ML models are described as black box models due to the complexity of its internal structure's mechanism. The Sobol' indices identify the most influential parameter and how much each parameter contributes to the variability in the model output. This important information could guide decision makers on understanding the groundwater resources to apply different scenarios and which parameter to prioritize and focus on. For example, our Sobol analysis showed that precipitation, ENSO and soil moisture have strong impacts on the groundwater storage change. Thus, one should suggest adopting rainwater harvesting and applying the managed aquifer recharge to recharge the depleted aquifers. The ENSO impact could give an early alert for decision makers to prepare for a heavy rainfall season and how to benefit with these rainfall amount. It is important to emphasize that the model structure significantly influences sensitivity to input variables and lag time. The inclusion of lag-6 in the RF model reflects its need for longer temporal information to capture the extended influences of ENSO and precipitation on groundwater variability. In contrast, lag-3 was sufficient for the LSTM model, which leverages its temporal memory capabilities to account for water retention dynamics in soil moisture. The variation in sensitivity highlights the differing responses of groundwater at various time scales, leading to distinct temporal sensitivity interpretations. This validates our model selection and enhances our understanding of regional dynamics.

According to the projections from the Intergovernmental Panel on Climate Change (IPCC), precipitation amount and frequence will be changed due to global warming (Le Treut et al., 2006). The projection of rainfall and temperature data for future could be used to forecast the groundwater level and assess the impact of climate change on the groundwater level variations. Groundwater is vulnerable to changes in temperature and precipitation due to climate change (Lam et al., 2021b). The increase in temperature will lead to an increase in the evaporation rates and could reduce the rainfall amount to recharge the aquifer. Recent studies have focused on applying ML and other modeling methods to forecast future groundwater level change under future climate projections (Dehghani et al., 2022; Ghazavi and Ebrahimi,

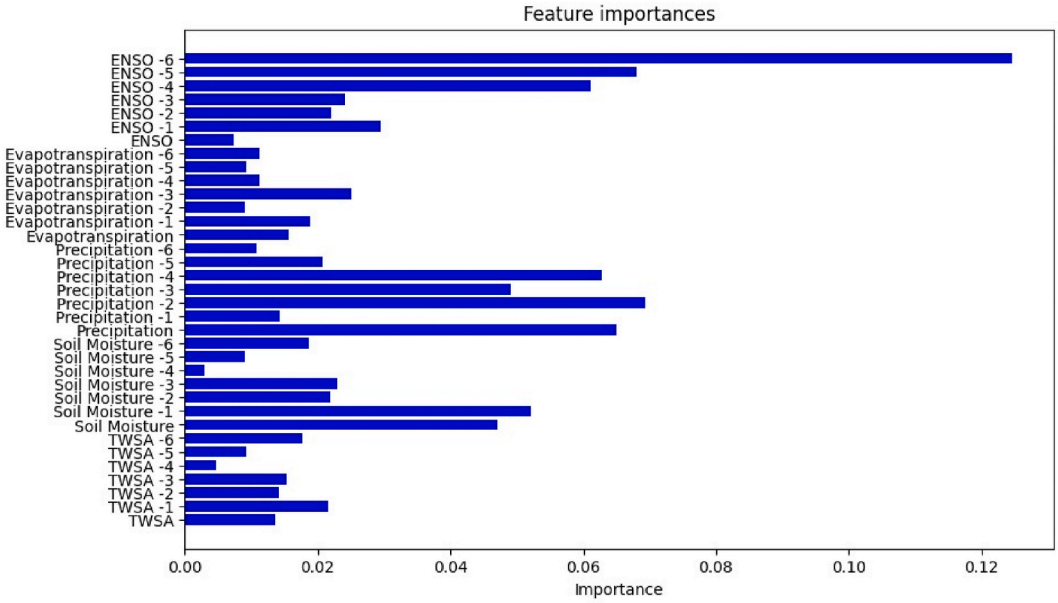

Fig. 10. Feature importance of predictors for groundwater level prediction using the Random Forest model. Results are based on the best model, incorporating inputs with a lag of up to 6 months.

2018; Lam et al., 2021b). The relationship between the climate change and groundwater storage is non-linear, however, in this research one can see the impact of climate change by increasing the temperature of the Pacific Ocean causing a change in rainfall and groundwater storage in Abu Dhabi Emirate.

5.2. Regional drivers of groundwater dynamics

It's important to note the complexity of recharge characteristics across the Abu Dhabi emirate, influenced by various factors such as soil variability, rainfall intensity, geology, topography, and rapid land use changes. For instance, the eastern region near Alain city experiences double the rainfall intensity compared to the western region (Alsharhan and Rizk, 2020). Sand dunes covering gravel plains can reduce aquifer recharge, while steep ground surfaces, especially in mountainous areas, result in minimal recharge rates (Sherif et al., 2018). Land use changes also play a significant role in recharge dynamics (Scanlon et al., 2006). Therefore, despite our regional-scale analysis, it's crucial to acknowledge substantial spatial variations in factors like land use, water availability, and groundwater level changes across our area of study. Rainfall distribution across the emirate varies significantly, with mountainous areas receiving approximately 160 mm annually compared to around 90 mm in coastal regions (Alsharhan and Rizk, 2020). Accordingly, to construct our regional groundwater model, we aggregated all remote sensing data products at the national scale. For an accurate representation of the spatial distribution in groundwater levels, future research should concentrate on formulating a spatially distributed model. Such a model would facilitate a more comprehensive understanding of groundwater dynamics in relation to climate, anthropogenic influences, and prospective changes. Additionally, localized analyses can clarify primary predictors of groundwater levels within specific regions, thereby offering valuable insights for future decision-making considerations.

The ENSO teleconnections significantly impact the precipitation patterns in the Arabian Peninsula. It has been observed that rainfall increased during the El Nino phases and drought conditions occurred during the La Nina Events (Felis et al., 2000). The El Nino phases can cause a shift in the atmospheric circulation resulting in more moisture moves from the Pacific to the Arabian Peninsula (Niranjan Kumar and Ouarda, 2014; Niranjan Kumar et al., 2016). Rainfall plays a critical role in recharging aquifers in the UAE. For example, studies have shown that rainfall events during the summer limit the aquifer recharge due to the high evaporation rate, while winter rainfall event could result in groundwater recharge (Sefelnasr et al., 2022). Imes and Wood (2007) demonstrated the impact of the thick high dunes on limiting the groundwater recharge even during heavy rainfall events. Based on the Carbon-14 dating method for various samples obtained from the Quaternary aquifer within the study areas, it is suggested that the source of water in the aquifer originates from rainfall periods between 32000 and 26000 years Before Present (BP) and between 9000 and 6000 years BP when annual rainfall was approximately 200 $\pm$ 50 mm (Wood and Imes, 2003; Woods and Imes, 1995). This supports our findings on the importance of ENSO as it controls the rainfall rate and intensity.

5.3. Limitations and sources of uncertainty

In our analysis, we primarily focus on deterministic modelling without an explicit consideration of model uncertainty, due to our broader interest in the influence of the selected variables on groundwater level change. However, our results are subject to various sources of uncertainty associated with our selected algorithms, including input data, model structure and optimization, and data aggregation methods. First, the input data did not encompass all relevant variables influencing groundwater levels, and inaccuracies or uncertainties in these datasets may propagate to the outputs, a factor that was not investigated. Second, optimization could be further refined by exploring a larger parameter space to potentially reach a global minimum. Lastly, the input data had varying spatial resolutions, which were aggregated to obtain regional values, potentially impacting the results.

In this study, the groundwater level variation was not smoothed to assess the performance of ML algorithms in detecting these sharp rises and declines. Future work should consider multiple parameters for a better performance. The UAE adopted desalination plants for the domestic supply. Recently, the Department of Energy in Abu Dhabi has connected the water networks to farms to reduce the groundwater pumping and preserve the groundwater resources. Furthermore, treated sewage water has been treated in UAE and distributed to farms two or three times a week. These water sources were not accounted in the calculation since data was not accessible. Due to the geological conditions in UAE, it has been estimated that irrigation return flow accounts

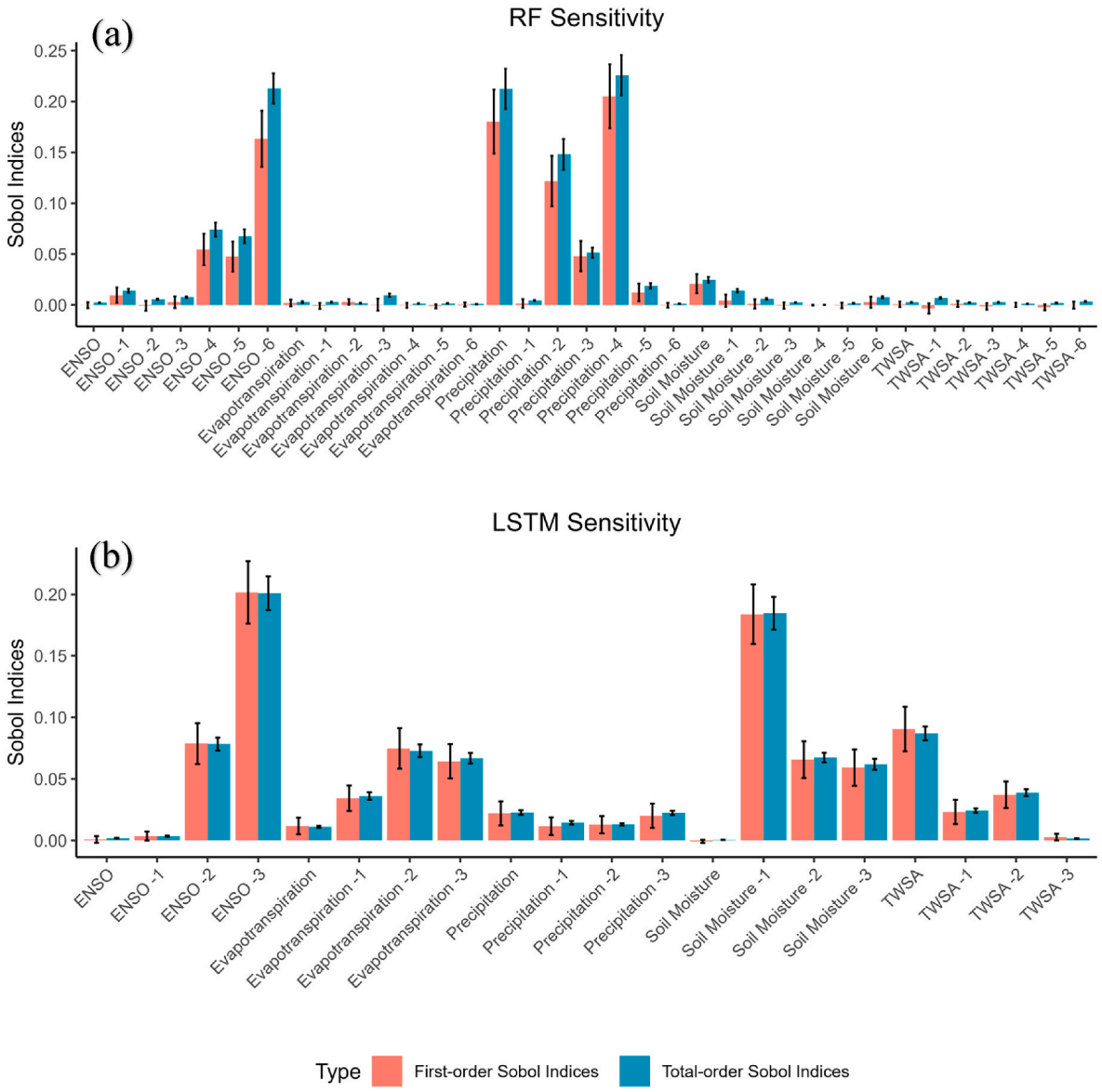

Fig. 11. (a) First order Sobol' indices and the total order Sobol' Indices for the variables with lags applied for (a) Random Forest model and (b) LSTM model, and the black lines represents the 95% confidence interval associated with each variable.

for 20% of the irrigation rate (Sherif et al., 2021). Since desalinated water (DSW) and treated sewage water (TSW) are used for irrigation, the soil moisture data could give an indication of recharge. Evidence of such an impact is observed by Sobol sensitivity analysis for the LSTM model as displayed in Fig. 11. The first order and total order Sobol method for the LSTM model showed a high score indicating the strong influence of soil moisture in the LSTM model. Additionally, the feature importance applied for the RF showed a similar outcome. The feature importance score has revealed that the second most important parameter is the soil moisture for the RF model. This indicates that aquifer recharge from DSW and TSW may have an impact on the groundwater. Thus, access to the DSW and TSW data could enhance the model's performance.

Oil production and produced water injection could also impact the analysis since GRACE accounts for water at all depths. This study did not include the produced water from the oil field in the model development. Access to wells in the oil field could improve the model and reduce the uncertainty in the calculations. This research data is obtained from 263 telemetric monitoring wells indicating the well-developed monitoring network established by the Environment agency of Abu Dhabi. This gave credibility and helped to develop an accurate model representing the aquifer dynamic of Abu Dhabi emirate.

5.4. *Prospects for future groundwater modeling*

Numerical modeling software has demonstrated satisfactory results in simulating groundwater flow across the Emirate (Sathish et al., 2018). However, to run these models in a transient mode, continuous temporal data on groundwater levels data, abstraction rates, rainfall and evapotranspiration are necessary. The dependency of numerical models on substantial data volumes could be a drawback and could be altered with data obtained from ML models to enhance the model performance, especially in the absence of continuous observational data. These continuous groundwater level timeseries developed from ML models could be used as an input in the conversion of numerical models in a steady state mode to a transient model. For example, the developed model in this study can be run easily by obtaining the freely available remote sensing data. These machine learning models can give important information of the aquifer dynamic in a fast time compared to the numerical models that require time and additional observation data. The timeseries obtained from the ML models could be used in numerical

models for developing a transient model or for the purpose of calibration and sensitivity analysis. However, these models connect the inputs to the outputs without providing insights into the internal processes underlying these relationships. This limitation, commonly associated with machine learning, has led to their characterization as "black box" models. This drawback can be addressed by utilizing "physics-informed" or "theory-guided" machine learning approaches, which constrain these models using physical characteristics and phenomena (Adombi et al., 2021).

A promising approach to reduce inaccuracies in current groundwater level simulations is to implement more advanced algorithms. Hybridizing existing models can enhance the performance of standalone models in predicting groundwater levels (Boo et al., 2024). For instance, CNN-LSTM models have recently gained considerable attention in hydrological applications (Ng et al., 2023). The convolutional neural network (CNN) component allows for the integration of spatially variable inputs, which contributes to greater heterogeneity and improved model reliability. Additionally, incorporating decomposition techniques helps to extract relevant features from input data, a key advantage given the highly nonlinear and non-stationary nature of groundwater systems (Maheswaran and Khosa, 2013).

While this study offers novel insights into groundwater level variability in the UAE, several promising directions have emerged for future research. A more spatially detailed study that incorporates groundwater heterogeneity is one such direction. Two key approaches to achieve this include downscaling GRACE data and developing grid-scale models. Although the TWSA data used in this study is coarse, downscaling techniques can enable higher-resolution analyses (Ali et al., 2024). These refined models could be especially useful in incorporating future climate scenarios, such as ENSO-related variability and broader climate change projections, which could significantly affect groundwater availability. By linking spatially distributed modeling with these climate scenarios, we can better capture the potential impacts of seasonal and long-term climate shifts on groundwater systems. Additionally, developing machine learning models for individual grid cells offers distinct advantages (Faruki Fahim et al., 2024). This approach allows for more spatially varied groundwater simulations, including local processes, and enables model extrapolation to grids without monitoring wells, thereby enhancing groundwater monitoring on a national scale.

6. Conclusion

Abu Dhabi Emirate is facing significant groundwater depletion, and the government is actively seeking solutions to preserve its groundwater resources. Regional environmental variables influence groundwater variability through complex interactions that are not yet well understood in the region. Gaining a better understanding of this variability, along with accurate modeling, is essential for more effective resource management and informed decision-making, particularly in the context of climate change challenges. The high cost for groundwater monitoring network maintenance and operation hinders water managers from having access to groundwater level change data. Alternatively, this research assessed the performance of remote sensing products coupled with machine learning techniques to predict the groundwater level. This study marks the first application of LSTM and RF models using satellite data and Earth observations in the Abu Dhabi Emirate. Furthermore, it is the first attempt to integrate ENSO into groundwater modeling in the UAE. We developed and evaluated the performance of two machine learning models, LSTM and RF, for regional groundwater level prediction. The developed LSTM model outperformed the RF model during the testing period.

A key finding in this research is the impact of the ENSO on groundwater level changes in the Abu Dhabi Emirate. The statistical metrics are acceptable to rely on the developed model. The LSTM's statistical metrics for the NSE, RMSE and R2 are 0.79, 0.38 m, and 0.79, respectively. The lags enhanced the LSTM and RF models significantly and the optimization techniques helped on demonstrating the influence of the lags. The Sobol global sensitivity analysis revealed a surprising outcome where among all the parameters derived from remote sensing products, the ENSO has the highest impact on the LSTM and RF models. This outcome implies the importance of considering the climate pattern and their impacts on the amount and variation of precipitation which eventually will impact the groundwater recharge. However, similar studies, both within the region and internationally, using traditional and advanced models, would be valuable for further comparison with our approach and findings. Finally, integrating remote sensing products into the LSTM and RF models can provide an acceptable groundwater level model.

CRediT authorship contribution statement

Khaled Alghafli: Writing – review & editing, Writing – original draft, Visualization, Validation, Methodology, Investigation, Formal analysis, Data curation, Conceptualization. **Xiaogang Shi:** Supervision, Methodology. **William Sloan:** Supervision. **Awad M. Ali:** Visualization, Methodology.

Declaration of competing interest

The authors declare that they have no known competing financial interests or personal relationships that could have appeared to influence the work reported in this paper.

Acknowledgements

The author acknowledges the Environment Agency of Abu Dhabi for providing the groundwater data from the telemetric monitoring network. The author also acknowledges the United Arab Emirates university and the Ministry of Higher Education for the PhD scholarship.

Appendix A. Supplementary data

Supplementary data to this article can be found online at https://doi.org/10.1016/j.gsd.2024.101389.

Data availability

The data that has been used is confidential.

References

Abid, M.A., Kucharski, F., Almazroui, M., Kang, I.S., 2016. Interannual rainfall variability and ECMWF-Sys4-based predictability over the Arabian Peninsula winter monsoon region. Q. J. R. Meteorol. Soc. 142 (694), 233–242.

Adiat, K., Ajayi, O., Akinlalu, A., Tijani, I., 2020. Prediction of groundwater level in basement complex terrain using artificial neural network: a case of Ijebu-Jesa, southwestern Nigeria. Appl. Water Sci. 10, 1–14.

Adombi, A.V.D.P., Chesnaux, R., Boucher, M.-A., 2021. Review: theory-guided machine learning applied to hydrogeology—state of the art, opportunities and future challenges. Hydrogeol. J. 29 (8), 2671–2683. https://doi.org/10.1007/s10040-021-02403-2.

Afrifa, S., Zhang, T., Appiahene, P., Varadarajan, V., 2022. Mathematical and machine learning models for groundwater level changes: a systematic review and bibliographic analysis. Future Internet. https://doi.org/10.3390/fi14090259.

Afzaal, H., Farooque, A.A., Abbas, F., Acharya, B., Esau, T., 2019. Groundwater estimation from major physical hydrology components using artificial neural networks and deep learning. Water 12 (1), 5.

Al-Bakri, J., 2016. Mapping Irrigated Crops and Estimation of Crop Water Consumption in Amman-Zarqa Basin A Report for Regional Coordination on Improved Water Resources Management and Capacity Building Ministry of Water and Irrigation. https://doi.org/10.13140/RG.2.2.34390.55368. Amman, Jordan.

AlEbri, M., Arman, H., Shalaby, A., 2016. The impact of el Niño and La niña on the United Arab Emirates (UAE) rainfall. General Scientific Research 4, 5–10.

Alghafli, K., et al., 2023a. Evaluation of runoff estimation from GRACE coupled with different meteorological gridded products over the Upper Blue Nile Basin. J. Hydrol.: Reg. Stud. 50, 101545. https://doi.org/10.1016/j.ejrh.2023.101545.

Alghafli, K., et al., 2023b. Groundwater recharge estimation using in-situ and GRACE observations in the eastern region of the United Arab Emirates. Sci. Total Environ. 867, 161489. https://doi.org/10.1016/j.scitotenv.2023.161489.
Ali, A.M., Melsen, L.A., Teuling, A.J., 2023. Inferring reservoir filling strategies under limited-data-availability conditions using hydrological modeling and Earth observations: the case of the Grand Ethiopian Renaissance Dam (GERD). Hydrol. Earth Syst. Sci. 27 (21), 4057–4086. https://doi.org/10.5194/hess-27-4057-2023.
Ali, M.Z., Chu, H.-J., Burbey, T.J., 2020. Mapping and predicting subsidence from spatio-temporal regression models of groundwater-drawdown and subsidence observations. Hydrogeol. J. 28 (8), 2865–2876. https://doi.org/10.1007/s10040-020-02211-0.
Ali, S., et al., 2022. Constructing high-resolution groundwater drought at spatio-temporal scale using GRACE satellite data based on machine learning in the Indus Basin. J. Hydrol. 612, 128295.
Ali, S., et al., 2024. Downscaled GRACE/GRACE-FO observations for spatial and temporal monitoring of groundwater storage variations at the local scale using machine learning. Groundwater for Sustainable Development 25, 101100. https://doi.org/10.1016/j.gsd.2024.101100.
Alley, W.M., Healy, R.W., LaBaugh, J.W., Reilly, T.E., 2002. Flow and storage in groundwater systems. Science 296 (5575), 1985–1990. https://doi.org/10.1126/science.1067123.
Almuhaylan, M.R., et al., 2020. Evaluating the impacts of pumping on aquifer depletion in arid regions using MODFLOW, ANFIS and ANN. Water. https://doi.org/10.3390/w12082297.
Alsharhan, A.S., Rizk, Z.E., 2020. Water resources and water demands in the UAE. In: Alsharhan, A.S., Rizk, Z.E. (Eds.), Water Resources and Integrated Management of the United Arab Emirates. Springer International Publishing, Cham, pp. 757–791. https://doi.org/10.1007/978-3-030-31684-6_27.
Atif, R.M., et al., 2020. Extreme precipitation events over Saudi Arabia during the wet season and their associated teleconnections. Atmos. Res. 231, 104655.
Baig, F., Abrar, M., Chen, H., Sherif, M., 2022. Rainfall consistency, variability, and concentration over the UAE: satellite precipitation products vs. Rain gauge observations. Rem. Sens. https://doi.org/10.3390/rs14225827.
Ballio, F., Guadagnini, A., 2004. Convergence assessment of numerical Monte Carlo simulations in groundwater hydrology. Water Resour. Res. 40 (4). https://doi.org/10.1029/2003WR002876.
Baroni, G., Scheiffele, L.M., Schrön, M., Ingwersen, J., Oswald, S.E., 2018. Uncertainty, sensitivity and improvements in soil moisture estimation with cosmic-ray neutron sensing. J. Hydrol. 564, 873–887. https://doi.org/10.1016/j.jhydrol.2018.07.053.
Baroni, G., Tarantola, S., 2014. A General Probabilistic Framework for uncertainty and global sensitivity analysis of deterministic models: a hydrological case study. Environ. Model. Software 51, 26–34.
Batista, L.V., et al., 2018. Groundwater and surface water connectivity within the recharge area of Guarani aquifer system during El Niño 2014–2016. Hydrol. Process. 32 (16), 2483–2495.
Beaudoing, H., Rodell, M., 2020a. GLDAS Noah land surface model L4 monthly 0.25 x 0.25 degree V2.1. In: NASA/GSFC/HSL. Goddard Earth Sciences Data and Information Services Center (GES DISC), Greenbelt, Maryland, USA. https://doi.org/10.5067/SXAVCZFAQLNO.
Beaudoing, H., Rodell, M., 2020b. GLDAS Noah Land Surface Model L4 Monthly 1.0 X 1.0 Degree V2.1. Goddard Earth Sciences Data and Information Services Center (GES DISC). https://doi.org/10.5067/LWTYSMP3VM5Z.
Beaudoing, H., Rodell, M., 2020c. GLDAS VIC Land Surface Model L4 Monthly 1.0 X 1.0 Degree V2.1. Goddard Earth Sciences Data and Information Services Center (GES DISC). https://doi.org/10.5067/VWTH7S6218SG.
Berthelin, R., et al., 2023. Estimating karst groundwater recharge from soil moisture observations – a new method tested at the Swabian Alb, southwest Germany. Hydrol. Earth Syst. Sci. 27 (2), 385–400. https://doi.org/10.5194/hess-27-385-2023.
Bhanja, S.N., Mukherjee, A., Saha, D., Velicogna, I., Famiglietti, J.S., 2016. Validation of GRACE based groundwater storage anomaly using in-situ groundwater level measurements in India. J. Hydrol. 543, 729–738.
Biau, G., Scornet, E., 2016. A random forest guided tour. TEST 25 (2), 197–227. https://doi.org/10.1007/s11749-016-0481-7.
Boo, K.B.W., et al., 2024. Groundwater level forecasting with machine learning models: a review. Water Res. 252, 121249. https://doi.org/10.1016/j.watres.2024.121249.
Bordbar, M., et al., 2022. Improving the coastal aquifers' vulnerability assessment using SCMAI ensemble of three machine learning approaches. Nat. Hazards 110 (3), 1799–1820. https://doi.org/10.1007/s11069-021-05013-z.
Borgonovo, E., Lu, X., Plischke, E., Rakovec, O., Hill, M.C., 2017. Making the most out of a hydrological model data set: sensitivity analyses to open the model black-box. Water Resour. Res. 53 (9), 7933–7950.
Boughriba, M., Jilali, A., 2018. Climate change and modeling of an unconfined aquifer: the Triffa plain, Morocco. Environ. Dev. Sustain. 20 (5), 2009–2026. https://doi.org/10.1007/s10668-017-9974-0.
Bouramtane, T., Leblanc, M., Kacimi, I., Ouatiki, H., Boudhar, A., 2023. The contribution of remote sensing and input feature selection for groundwater level prediction using LSTM neural networks in the Oum Er-Rbia Basin, Morocco. Frontiers in Water 5, 1241451.
Bowes, B.D., Sadler, J.M., Morsy, M.M., Behl, M., Goodall, J.L., 2019. Forecasting groundwater table in a flood prone coastal city with long short-term memory and recurrent neural networks. Water 11 (5), 1098.
Breiman, L., 2001. Random forests. Mach. Learn. 45, 5–32.
Brunner, P., Simmons, C.T., 2012. HydroGeoSphere: a fully integrated, physically based hydrological model. Groundwater 50 (2), 170–176. https://doi.org/10.1111/j.1745-6584.2011.00882.x.
Cai, H., Shi, H., Liu, S., Babovic, V., 2021. Impacts of regional characteristics on improving the accuracy of groundwater level prediction using machine learning: the case of central eastern continental United States. J. Hydrol.: Reg. Stud. 37, 100930.
Capotondi, A., et al., 2015. Understanding ENSO diversity. Bull. Am. Meteorol. Soc. 96 (6), 921–938. https://doi.org/10.1175/BAMS-D-13-00117.1.
Chang, F.-J., Chang, L.-C., Huang, C.-W., Kao, I.-F., 2016. Prediction of monthly regional groundwater levels through hybrid soft-computing techniques. J. Hydrol. 541, 965–976.
Chen, C., He, W., Zhou, H., Xue, Y., Zhu, M., 2020. A comparative study among machine learning and numerical models for simulating groundwater dynamics in the Heihe River Basin, northwestern China. Sci. Rep. 10 (1), 3904. https://doi.org/10.1038/s41598-020-60698-9.
Chen, H., Zhang, W., Nie, N., Guo, Y., 2019. Long-term groundwater storage variations estimated in the Songhua River Basin by using GRACE products, land surface models, and in-situ observations. Sci. Total Environ. 649, 372–387.
Chen, L.-H., Chen, C.-T., Pan, Y.-G., 2010. Groundwater level prediction using SOM-RBFN multisite model. J. Hydrol. Eng. 15 (8), 624–631.
Cobaner, M., Babayigit, B., Dogan, A., 2016. Estimation of groundwater levels with surface observations via genetic programming. Journal-American Water Works Association 108 (6), E335–E348.
Cooley, R.L., 1997. Confidence intervals for ground-water models using linearization, likelihood, and bootstrap methods. Groundwater 35 (5), 869–880. https://doi.org/10.1111/j.1745-6584.1997.tb00155.x.
Cooley, R.L., Naff, R.L., 1990. Regression Modeling of Ground-Water Flow.
Coppola, E., Szidarovszky, F., Poulton, M., Charles, E., 2003. Artificial neural network approach for predicting transient water levels in a multilayered groundwater system under variable state, pumping, and climate conditions. J. Hydrol. Eng. 8 (6), 348–360. https://doi.org/10.1061/(ASCE)1084-0699(2003)8:6(348).
Coulibaly, P., Anctil, F., Aravena, R., Bobée, B., 2001. Artificial neural network modeling of water table depth fluctuations. Water Resour. Res. 37 (4), 885–896. https://doi.org/10.1029/2000WR900368.
Dangar, S., Asoka, A., Mishra, V., 2021. Causes and implications of groundwater depletion in India: a review. J. Hydrol. 596, 126103. https://doi.org/10.1016/j.jhydrol.2021.126103.
Dax, A., Zilberbrand, M., 2018. Imputing missing groundwater observations. Nord. Hydrol 49 (3), 831–845.
De Filippis, G., Margiotta, S., Caruso, F., Negri, S.L., 2020. Open questions about the hydrodynamic behaviour of the deep, coastal aquifer of the Salento peninsula (south-eastern Italy): coupling expert knowledge, data, and numerical modelling for testing hydrogeological conceptual models. Sci. Total Environ. 715, 136962. https://doi.org/10.1016/j.scitotenv.2020.136962.
Dehghani, R., Poudeh, H.T., Izadi, Z., 2022. The effect of climate change on groundwater level and its prediction using modern meta-heuristic model. Groundwater for Sustainable Development 16, 100702. https://doi.org/10.1016/j.gsd.2021.100702.
Derbela, M., Nouiri, I., 2020. Intelligent approach to predict future groundwater level based on artificial neural networks (ANN). Euro-Mediterranean Journal for Environmental Integration 5, 1–11.
Di Nunno, F., Granata, F., 2020. Groundwater level prediction in Apulia region (Southern Italy) using NARX neural network. Environ. Res. 190, 110062. https://doi.org/10.1016/j.envres.2020.110062.
Diersch, H.-J.G., 2014. Flow in saturated porous media: groundwater flow. In: Diersch, H.-J.G. (Ed.), FEFLOW: Finite Element Modeling of Flow, Mass and Heat Transport in Porous and Fractured Media. Springer Berlin Heidelberg, Berlin, Heidelberg, pp. 405–444. https://doi.org/10.1007/978-3-642-38739-5_9.
Ding, J., Zhu, Q., 2022. The accuracy of multisource evapotranspiration products and their applicability in streamflow simulation over a large catchment of Southern China. J. Hydrol.: Reg. Stud. 41, 101092. https://doi.org/10.1016/j.ejrh.2022.101092.
Diro, G.T., Toniazzo, T., Shaffrey, L., 2011. Ethiopian rainfall in climate models. African Climate and Climate Change: Physical, Social and Political Perspectives, pp. 51–69.
Döll, P., et al., 2012. Impact of water withdrawals from groundwater and surface water on continental water storage variations. J. Geodyn. 59–60, 143–156. https://doi.org/10.1016/j.jog.2011.05.001.
Duchi, J., Hazan, E., Singer, Y., 2011. Adaptive subgradient methods for online learning and stochastic optimization. Journal of machine learning research 12 (7).
Dwivedi, D., et al., 2022. Imputation of contiguous gaps and extremes of subhourly groundwater time series using random forests. Journal of Machine Learning for Modeling and Computing 3 (2).
El-Azhari, A., et al., 2024. Analyses of groundwater level in a data-scarce region based on assessed precipitation products and machine learning. Groundwater for Sustainable Development 26, 101299. https://doi.org/10.1016/j.gsd.2024.101299.
El Yaouti, F., El Mandour, A., Khattach, D., Kaufmann, O., 2008. Modelling groundwater flow and advective contaminant transport in the Bou-Areg unconfined aquifer (NE Morocco). Journal of Hydro-environment Research 2 (3), 192–209. https://doi.org/10.1016/j.jher.2008.08.003.
Fallah-Mehdipour, E., Haddad, O.B., Mariño, M., 2013. Prediction and simulation of monthly groundwater levels by genetic programming. Journal of Hydro-Environment Research 7 (4), 253–260.
Faruki Fahim, A.K., Kamal, A.S.M.M., Shahid, S., 2024. Modeling spatial groundwater level patterns of Bangladesh using physio-climatic variables and machine learning algorithms. Groundwater for Sustainable Development 25, 101142. https://doi.org/10.1016/j.gsd.2024.101142.
Felis, T., et al., 2000. A coral oxygen isotope record from the northern Red Sea documenting NAO, ENSO, and North Pacific teleconnections on Middle East climate variability since the year 1750. Paleoceanography 15 (6), 679–694. https://doi.org/10.1029/1999PA000477.

Feng, F., Ghorbani, H., Radwan, A.E., 2024. Predicting groundwater level using traditional and deep machine learning algorithms. Front. Environ. Sci. 12.
Feng, S., Kang, S., Huo, Z., Chen, S., Mao, X., 2008. Neural networks to simulate regional ground water levels affected by human activities. Groundwater 46 (1), 80–90. https://doi.org/10.1111/j.1745-6584.2007.00366.x.
Feng, W., et al., 2013. Evaluation of groundwater depletion in North China using the Gravity Recovery and Climate Experiment (GRACE) data and ground-based measurements. Water Resour. Res. 49 (4), 2110–2118.
Fleming, S.W., Quilty, E.J., 2006. Aquifer responses to el Niño–Southern oscillation, southwest British Columbia. Groundwater 44 (4), 595–599.
Funk, C., et al., 2015. The climate hazards infrared precipitation with stations—a new environmental record for monitoring extremes. Sci. Data 2 (1), 150066. https://doi.org/10.1038/sdata.2015.66.
Gao, Y., Du, E., Yi, S., Han, Y., Zheng, C., 2022. An improved numerical model for groundwater flow simulation with MPFA method on arbitrary polygon grids. J. Hydrol. 606, 127399. https://doi.org/10.1016/j.jhydrol.2021.127399.
Gers, F.A., Schmidhuber, J., Cummins, F., 2000. Learning to forget: continual prediction with LSTM. Neural Comput. 12 (10), 2451–2471. https://doi.org/10.1162/089976600300015015.
Gharehbaghi, A., Ghasemlounia, R., Ahmadi, F., Albaji, M., 2022. Groundwater level prediction with meteorologically sensitive Gated Recurrent Unit (GRU) neural networks. J. Hydrol. 612, 128262.
Ghazavi, R., Ebrahimi, H., 2018. Predicting the impacts of climate change on groundwater recharge in an arid environment using modeling approach. International Journal of Climate Change Strategies and Management 11 (1), 88–99.
Gleeson, T., et al., 2010. Groundwater sustainability strategies. Nat. Geosci. 3 (6), 378–379.
Gleixner, S., Keenlyside, N., Viste, E., Korecha, D., 2017. The El Niño effect on Ethiopian summer rainfall. Clim. Dynam. 49 (5), 1865–1883. https://doi.org/10.1007/s00382-016-3421-z.
Gong, X., Geng, J., Sun, Q., Gu, C., Zhang, W., 2020. Experimental study on pumping-induced land subsidence and earth fissures: a case study in the Su-Xi-Chang region, China. Bull. Eng. Geol. Environ. 79 (9), 4515–4525. https://doi.org/10.1007/s10064-020-01864-1.
Gropius, M., et al., 2022. Estimation of unrecorded groundwater abstractions in Jordan through regional groundwater modelling. Hydrogeol. J. 30 (6), 1769–1787. https://doi.org/10.1007/s10040-022-02523-3.
Gupta, B., Nema, A., Mittal, A., Maurya, N., 2003. Modeling of Groundwater Systems: Problems and Pitfalls, pp. 87–97.
Hamman, J.J., Nijssen, B., Bohn, T.J., Gergel, D.R., Mao, Y., 2018. The Variable Infiltration Capacity model version 5 (VIC-5): infrastructure improvements for new applications and reproducibility. Geosci. Model Dev. (GMD) 11 (8), 3481–3496. https://doi.org/10.5194/gmd-11-3481-2018.
Hanasaki, N., Yoshikawa, S., Pokhrel, Y., Kanae, S., 2018. A global hydrological simulation to specify the sources of water used by humans. Hydrol. Earth Syst. Sci. 22 (1), 789–817. https://doi.org/10.5194/hess-22-789-2018.
Harbaugh, A.W., 2005. MODFLOW-2005 : the U.S. Geological Survey modular ground-water model–the ground-water flow process 6–A16. https://doi.org/10.3133/tm6A16.
Healy, R.W., 2010. Estimating Groundwater Recharge. Cambridge University Press. https://doi.org/10.1017/CBO9780511780745.
Hinton, G.E., Srivastava, N., Krizhevsky, A., Sutskever, I., Salakhutdinov, R.R., 2012. Improving neural networks by preventing co-adaptation of feature detectors. arXiv preprint arXiv:1207.0580.
Hochreiter, S., Schmidhuber, J., 1997. Long short-term memory. Neural Comput. 9, 1735–1780. https://doi.org/10.1162/neco.1997.9.8.1735.
Højberg, A.L., Refsgaard, J.C., 2005. Model uncertainty – parameter uncertainty versus conceptual models. Water Sci. Technol. 52 (6), 177–186. https://doi.org/10.2166/wst.2005.0166.
Horan, M.F., et al., 2023. Moisture sources for precipitation variability over the Arabian Peninsula. Clim. Dynam. 61 (9), 4793–4807. https://doi.org/10.1007/s00382-023-06762-2.
Huang, Z., et al., 2015. Subregional-scale groundwater depletion detected by GRACE for both shallow and deep aquifers in North China Plain. Geophys. Res. Lett. 42 (6), 1791–1799. https://doi.org/10.1002/2014GL062498.
Hund, S.V., Grossmann, I., Steyn, D.G., Allen, D.M., Johnson, M.S., 2021. Changing water resources under el Niño, climate change, and growing water demands in seasonally dry tropical watersheds. Water Resour. Res. 57 (11), e2020WR028535. https://doi.org/10.1029/2020WR028535.
Imes, J.L., Wood, W.W., 2007. Solute and isotope constraint of groundwater recharge simulation in an arid environment, Abu Dhabi Emirate, United Arab Emirates. Hydrogeol. J. 15 (7), 1307–1315. https://doi.org/10.1007/s10040-007-0177-x.
Izady, A., et al., 2014. A framework toward developing a groundwater conceptual model. Arabian J. Geosci. 7, 3611–3631.
Jeong, J., Park, E., 2019. Comparative applications of data-driven models representing water table fluctuations. J. Hydrol. 572, 261–273.
Joseph, F.J.J., Nonsiri, S., Monsakul, A., 2021. Correction to: Keras and TensorFlow: a hands-on experience. In: Prakash, K.B., Kannan, R., Alexander, S.A., Kanagachidambaresan, G.R. (Eds.), Advanced Deep Learning for Engineers and Scientists: A Practical Approach. Springer International Publishing, Cham, p. C1. https://doi.org/10.1007/978-3-030-66519-7_12. C1.
Kalu, I., Ndehedehe, C.E., Okwuashi, O., Eyoh, A.E., Ferreira, V.G., 2022. A new modelling framework to assess changes in groundwater level. J. Hydrol.: Reg. Stud. 43, 101185. https://doi.org/10.1016/j.ejrh.2022.101185.
Kang, H., 2013. The prevention and handling of the missing data. Korean journal of anesthesiology 64 (5), 402.
Kasiviswanathan, K., Saravanan, S., Balamurugan, M., Saravanan, K., 2016. Genetic programming based monthly groundwater level forecast models with uncertainty quantification. Modeling Earth Systems and Environment 2, 1–11.
Khaledi-Alamdari, M., Majnooni-Heris, A., Fakheri-Fard, A., Moghaddam, A.A., 2022. Modeling the impacts of various managerial scenarios on groundwater level raising in a coastal aquifer. Arabian J. Geosci. 15 (8), 695. https://doi.org/10.1007/s12517-022-09925-3.
Khazaz, L., Oulidi, H.J., El Moutaki, S., Ghafiri, A., 2015. Comparing and evaluating probabilistic and deterministic spatial interpolation methods for groundwater level of Haouz in Morocco. J. Geogr. Inf. Syst. 7 (6), 631.
Khorrami, B., Ali, S., Gündüz, O., 2023. Investigating the local-scale fluctuations of groundwater storage by using downscaled GRACE/GRACE-FO JPL mascon product Based on Machine Learning (ML) Algorithm. Water Resour. Manag. 1–18.
Kingma, D.P., Ba, J., 2014. Adam: a method for stochastic optimization. arXiv preprint arXiv:1412.6980.
Kochhar, A., Singh, H., Sahoo, S., Litoria, P.K., Pateriya, B., 2022. Prediction and forecast of pre-monsoon and post-monsoon groundwater level: using deep learning and statistical modelling. Modeling Earth Systems and Environment 8 (2), 2317–2329. https://doi.org/10.1007/s40808-021-01235-z.
Kolusu, S.R., et al., 2019. The El Niño event of 2015–2016: climate anomalies and their impact on groundwater resources in East and Southern Africa. Hydrol. Earth Syst. Sci. 23 (3), 1751–1762.
Lallahem, S., Mania, J., Hani, A., Najjar, Y., 2005. On the use of neural networks to evaluate groundwater levels in fractured media. J. Hydrol. 307 (1), 92–111. https://doi.org/10.1016/j.jhydrol.2004.10.005.
Lam, C.K.C., Lee, H., Yang, S.-R., Park, S., 2021a. A review on the significance and perspective of the numerical simulations of outdoor thermal environment. Sustain. Cities Soc. 71, 102971.
Lam, Q., Meon, G., Pätsch, M., 2021b. Coupled modelling approach to assess effects of climate change on a coastal groundwater system. Groundwater for Sustainable Development 14, 100633.
Lawrence, S., Giles, C.L., Tsoi, A.C., Back, A.D., 1997. Face recognition: a convolutional neural-network approach. IEEE Trans. Neural Network. 8 (1), 98–113.
Le Treut, H., et al., 2006. Historical overview of climate change science. IPCC 4RG.
Li, B., Beaudoing, H., Rodell, M., 2018. GLDAS catchment land surface model L4 daily 0.25 x 0.25 degree V2.0. In: NASA/GSFC/HSL. Goddard Earth Sciences Data and Information Services Center (GES DISC), Greenbelt, Maryland, USA. https://doi.org/10.5067/LYHA9088MFWQ.
Li, B., Rodell, M., Sheffield, J., Wood, E., Sutanudjaja, E., 2019. Long-term, non-anthropogenic groundwater storage changes simulated by three global-scale hydrological models. Sci. Rep. 9 (1), 10746. https://doi.org/10.1038/s41598-019-47219-z.
Liu, D., Mishra, A.K., Yu, Z., Lü, H., Li, Y., 2021. Support vector machine and data assimilation framework for Groundwater Level Forecasting using GRACE satellite data. J. Hydrol. 603, 126929. https://doi.org/10.1016/j.jhydrol.2021.126929.
Long, D., et al., 2020. South-to-North Water Diversion stabilizing Beijing's groundwater levels. Nat. Commun. 11 (1), 3665. https://doi.org/10.1038/s41467-020-17428-6.
Maheswaran, R., Khosa, R., 2013. Long term forecasting of groundwater levels with evidence of non-stationary and nonlinear characteristics. Comput. Geosci. 52, 422–436. https://doi.org/10.1016/j.cageo.2012.09.030.
Makler-Pick, V., Gal, G., Gorfine, M., Hipsey, M.R., Carmel, Y., 2011. Sensitivity analysis for complex ecological models – a new approach. Environ. Model. Software 26 (2), 124–134. https://doi.org/10.1016/j.envsoft.2010.06.010.
Malakar, P., et al., 2021. Machine-learning-based regional-scale groundwater level prediction using GRACE. Hydrogeol. J. 29 (3), 1027–1042. https://doi.org/10.1007/s10040-021-02306-2.
Martens, B., et al., 2017. GLEAM v3: satellite-based land evaporation and root-zone soil moisture. Geosci. Model Dev. (GMD) 10 (5), 1903–1925. https://doi.org/10.5194/gmd-10-1903-2017.
Masafu, C., Williams, R., 2024. Satellite video remote sensing for flood model validation. Water Resour. Res. 60 (1), e2023WR034545. https://doi.org/10.1029/2023WR034545.
Mathias, S.A., Sorensen, J.P.R., Butler, A.P., 2017. Soil moisture data as a constraint for groundwater recharge estimation. J. Hydrol. 552, 258–266. https://doi.org/10.1016/j.jhydrol.2017.06.040.
Miralles, D.G., et al., 2011. Global land-surface evaporation estimated from satellite-based observations. Hydrol. Earth Syst. Sci. 15 (2), 453–469. https://doi.org/10.5194/hess-15-453-2011.
Mohammadi, K., 2008. Groundwater table estimation using MODFLOW and artificial neural networks. In: Abrahart, R.J., See, L.M., Solomatine, D.P. (Eds.), Practical Hydroinformatics: Computational Intelligence and Technological Developments in Water Applications. Springer, Berlin Heidelberg, Berlin, Heidelberg, pp. 127–138. https://doi.org/10.1007/978-3-540-79881-1_10.
Moravej, M., Amani, P., Hosseini-Moghari, S.-M., 2020. Groundwater level simulation and forecasting using interior search algorithm-least square support vector regression (ISA-LSSVR). Groundwater for Sustainable Development 11, 100447.
Mukherjee, A., Ramachandran, P., 2018. Prediction of GWL with the help of GRACE TWS for unevenly spaced time series data in India : analysis of comparative performances of SVR, ANN and LRM. J. Hydrol. 558, 647–658. https://doi.org/10.1016/j.jhydrol.2018.02.005.
Müller, J., et al., 2021. Surrogate optimization of deep neural networks for groundwater predictions. J. Global Optim. 81, 203–231.
Ng, K.W., et al., 2023. A review of hybrid deep learning applications for streamflow forecasting. J. Hydrol. 625, 130141. https://doi.org/10.1016/j.jhydrol.2023.130141.

Nikolos, I.K., Stergiadi, M., Papadopoulou, M.P., Karatzas, G.P., 2008. Artificial neural networks as an alternative approach to groundwater numerical modelling and environmental design. Hydrol. Process. 22 (17), 3337–3348. https://doi.org/10.1002/hyp.6916.
Niranjan Kumar, K., Ouarda, T., 2014. Precipitation variability over UAE and global SST teleconnections. J. Geophys. Res. Atmos. 119 (17), 322, 10,313-10.
Niranjan Kumar, K., Ouarda, T.B.M.J., Sandeep, S., Ajayamohan, R.S., 2016. Wintertime precipitation variability over the Arabian Peninsula and its relationship with ENSO in the CAM4 simulations. Clim. Dynam. 47 (7), 2443–2454. https://doi.org/10.1007/s00382-016-2973-2.
Nourani, V., et al., 2024. Application of the machine learning methods for GRACE data based groundwater modeling, a systematic review. Groundwater for Sustainable Development 25, 101113. https://doi.org/10.1016/j.gsd.2024.101113.
O'Reilly, A.M., Holt, R.M., Davidson, G.R., Patton, Austin C., Rigby, J.R., 2020. A dynamic water balance/nonlinear reservoir model of a perched phreatic aquifer–river system with hydrogeologic threshold effects. Water Resour. Res. 56 (6), e2019WR025382. https://doi.org/10.1029/2019WR025382.
Oikonomou, P.D., Alzraiee, A.H., Karavitis, C.A., Waskom, R.M., 2018. A novel framework for filling data gaps in groundwater level observations. Adv. Water Resour. 119, 111–124. https://doi.org/10.1016/j.advwatres.2018.06.008.
Parkin, G., Birkinshaw, S.J., Younger, P.L., Rao, Z., Kirk, S., 2007. A numerical modelling and neural network approach to estimate the impact of groundwater abstractions on river flows. J. Hydrol. 339 (1), 15–28. https://doi.org/10.1016/j.jhydrol.2007.01.041.
Patra, S.R., Chu, H.-J., Tatas, 2023. Regional groundwater sequential forecasting using global and local LSTM models. J. Hydrol.: Reg. Stud. 47, 101442. https://doi.org/10.1016/j.ejrh.2023.101442.
Pedregosa, F., et al., 2011. Scikit-learn: machine learning in Python. the Journal of machine Learning research 12, 2825–2830.
Rajaee, T., Ebrahimi, H., Nourani, V., 2019. A review of the artificial intelligence methods in groundwater level modeling. J. Hydrol. 572, 336–351. https://doi.org/10.1016/j.jhydrol.2018.12.037.
Ratto, M., et al., 2007. Uncertainty, sensitivity analysis and the role of data based mechanistic modeling in hydrology. Hydrol. Earth Syst. Sci. 11 (4), 1249–1266.
Rayner, N.A., et al., 2003. Global analyses of sea surface temperature, sea ice, and night marine air temperature since the late nineteenth century. J. Geophys. Res. Atmos. 108 (D14). https://doi.org/10.1029/2002JD002670.
Rodell, M., et al., 2004. The global land data assimilation system. Bull. Am. Meteorol. Soc. 85 (3), 381–394. https://doi.org/10.1175/BAMS-85-3-381.
Rodell, M., Velicogna, I., Famiglietti, J.S., 2009. Satellite-based estimates of groundwater depletion in India. Nature 460 (7258), 999–1002.
Rodriguez-Galiano, V., Sanchez-Castillo, M., Chica-Olmo, M., Chica-Rivas, M., 2015. Machine learning predictive models for mineral prospectivity: an evaluation of neural networks, random forest, regression trees and support vector machines. Ore Geol. Rev. 71, 804–818. https://doi.org/10.1016/j.oregeorev.2015.01.001.
Rojas, R., Feyen, L., Dassargues, A., 2008. Conceptual model uncertainty in groundwater modeling: combining generalized likelihood uncertainty estimation and Bayesian model averaging. Water Resour. Res. 44 (12). https://doi.org/10.1029/2008WR006908.
Ropelewski, C.F., Halpert, M.S., 1986. North American precipitation and temperature patterns associated with the El Niño/Southern Oscillation (ENSO). Mon. Weather Rev. 114 (12), 2352–2362.
Rosolem, R., Gupta, H.V., Shuttleworth, W.J., Zeng, X., de Gonçalves, L.G.G., 2012. A fully multiple-criteria implementation of the Sobol' method for parameter sensitivity analysis. J. Geophys. Res. Atmos. 117 (D7). https://doi.org/10.1029/2011JD016355.
Rumelhart, D.E., Hinton, G.E., Williams, R.J., 1986. Learning representations by back-propagating errors. Nature 323 (6088), 533–536. https://doi.org/10.1038/323533a0.
Sadeghi, M., et al., 2019. Evaluation of PERSIANN-CDR constructed using GPCP V2. 2 and V2. 3 and a comparison with TRMM 3B42 V7 and CPC unified gauge-based analysis in global scale. Rem. Sens. 11 (23), 2755.
Sadeghi, M., et al., 2021. PERSIANN-CCS-CDR, a 3-hourly 0.04° global precipitation climate data record for heavy precipitation studies. Sci. Data 8 (1), 157. https://doi.org/10.1038/s41597-021-00940-9.
Sahoo, S., Jha, M.K., 2013. Groundwater-level prediction using multiple linear regression and artificial neural network techniques: a comparative assessment. Hydrogeol. J. 21 (8), 1865–1887. https://doi.org/10.1007/s10040-013-1029-5.
Sahoo, S., Russo, T.A., Elliott, J., Foster, I., 2017. Machine learning algorithms for modeling groundwater level changes in agricultural regions of the U.S. Water Resour. Res. 53 (5), 3878–3895. https://doi.org/10.1002/2016WR019933.
Sahu, R.K., et al., 2020. Impact of input feature selection on groundwater level prediction from a multi-layer perceptron neural network. Frontiers in Water 2.
Salas, J.D., 1980. Applied Modeling of Hydrologic Time Series. Water Resources Publication.
Salas, J.D., 1993. Analysis and modelling of hydrological time series. Handbook of hydrology 19.
Samani, S., 2024. Unraveling aquifer dynamics: time series evaluation for informed groundwater management. Groundwater for Sustainable Development 25, 101174. https://doi.org/10.1016/j.gsd.2024.101174.
Samani, S., Vadiati, M., Azizi, F., Zamani, E., Kisi, O., 2022. Groundwater level simulation using soft computing methods with emphasis on major meteorological components. Water Resour. Manag. 36 (10), 3627–3647. https://doi.org/10.1007/s11269-022-03217-x.
Sarkar, H., Goriwale, S.S., Ghosh, J.K., Ojha, C.S.P., Ghosh, S.K., 2024. Potential of machine learning algorithms in groundwater level prediction using temporal gravity data. Groundwater for Sustainable Development 25, 101114. https://doi.org/10.1016/j.gsd.2024.101114.
Sathish, S., Mohamed, M., Klammler, H., 2018. Regional groundwater flow model for Abu Dhabi Emirate: scenario-based investigation. Environ. Earth Sci. 77 (11), 409. https://doi.org/10.1007/s12665-018-7544-x.
Scanlon, B.R., et al., 2012. Groundwater depletion and sustainability of irrigation in the US high plains and central valley. Proc. Natl. Acad. Sci. USA 109 (24), 9320–9325.
Scanlon, B.R., et al., 2006. Global synthesis of groundwater recharge in semiarid and arid regions. Hydrol. Process. 20 (15), 3335–3370. https://doi.org/10.1002/hyp.6335.
Sefelnasr, A., et al., 2022. Enhancement of groundwater recharge from wadi Al bih dam. UAE, Water. https://doi.org/10.3390/w14213448.
Seyoum, W.M., Kwon, D., Milewski, A.M., 2019. Downscaling GRACE TWSA data into high-resolution groundwater level anomaly using machine learning-based models in a glacial aquifer system. Rem. Sens. 11 (7), 824.
Shamsudduha, M., Taylor, R., Longuevergne, L., 2012. Monitoring groundwater storage changes in the highly seasonal humid tropics: validation of GRACE measurements in the Bengal Basin. Water Resour. Res. 48 (2).
Shamsudduha, M., Taylor, R.G., 2020. Groundwater storage dynamics in the world's large aquifer systems from GRACE: uncertainty and role of extreme precipitation. Earth Syst. Dynam. 11 (3), 755–774. https://doi.org/10.5194/esd-11-755-2020.
Shen, M., et al., 2015. Evaporative cooling over the Tibetan Plateau induced by vegetation growth. Proc. Natl. Acad. Sci. USA 112 (30), 9299–9304. https://doi.org/10.1073/pnas.1504418112.
Sherif, M., et al., 2021. Spatial and temporal changes of groundwater storage in the quaternary aquifer, UAE. Water. https://doi.org/10.3390/w13060864.
Sherif, M.M., Ebraheem, A.M., Al Mulla, M.M., Shetty, A.V., 2018. New system for the assessment of annual groundwater recharge from rainfall in the United Arab Emirates. Environ. Earth Sci. 77 (11), 412. https://doi.org/10.1007/s12665-018-7591-3.
Shukla, J., Mintz, Y., 1982. Influence of land-surface evapotranspiration on the earth's climate. Science 215 (4539), 1498–1501. https://doi.org/10.1126/science.215.4539.1498.
Siebert, S., et al., 2010. Groundwater use for irrigation – a global inventory. Hydrol. Earth Syst. Sci. 14 (10), 1863–1880. https://doi.org/10.5194/hess-14-1863-2010.
Sikdar, P.K., 2019. Numerical groundwater modelling. In: Sikdar, P.K. (Ed.), Groundwater Development and Management: Issues and Challenges in South Asia. Springer International Publishing, Cham, pp. 191–207. https://doi.org/10.1007/978-3-319-75115-3_7.
Smith, M., Cross, K., Paden, M., Laban, P., 2016. Spring–Managing Groundwater Sustainably. IUCN, Gland, Switzerland.
Sobol, I.y.M., 1990. On sensitivity estimation for nonlinear mathematical models. Matematicheskoe modelirovanie 2 (1), 112–118.
Soboĺ, I., 1993. Sensitivity estimates for nonlinear mathematical models. Math. Model. Comput. Exp. 1, 407.
Solgi, R., Loáiciga, H.A., Kram, M., 2021. Long short-term memory neural network (LSTM-NN) for aquifer level time series forecasting using in-situ piezometric observations. J. Hydrol. 601, 126800. https://doi.org/10.1016/j.jhydrol.2021.126800.
Song, X., et al., 2015. Global sensitivity analysis in hydrological modeling: review of concepts, methods, theoretical framework, and applications. Journal of hydrology (Amsterdam) 523 (C), 739–757. https://doi.org/10.1016/j.jhydrol.2015.02.013.
Sorensen, J.P., et al., 2021. A influência da captação da água subterrâneas na interpretação de controles climáticos e eventos de recarga extremos em hidrogramas de poços no semiárido do Sul da África. Hydrogeol. J. 29, 2773–2787.
Sorooshian, S., Hsu, K., Braithwaite, D., Ashouri, H., 2014. NOAA climate data record (CDR) of precipitation estimation from remotely sensed information using artificial neural networks (PERSIANN-CDR), Version 1, Revision 1 gis. ncdc. noaa. gov/geoportal/catalog/search/resource/details. page.
Su, X., et al., 2017. Responses of groundwater vulnerability to groundwater extraction reduction in the Hun River Basin, northeastern China. Hum. Ecol. Risk Assess. 23 (5), 1121–1139. https://doi.org/10.1080/10807039.2017.1300858.
Sulaiman, A., et al., 2023. Peatland groundwater level in the Indonesian maritime continent as an alert for El Niño and moderate positive Indian Ocean dipole events. Sci. Rep. 13 (1), 939.
Sun, A.Y., 2013. Predicting groundwater level changes using GRACE data. Water Resour. Res. 49 (9), 5900–5912. https://doi.org/10.1002/wrcr.20421.
Sun, J., Hu, L., Li, D., Sun, K., Yang, Z., 2022. Data-driven models for accurate groundwater level prediction and their practical significance in groundwater management. J. Hydrol. 608, 127630. https://doi.org/10.1016/j.jhydrol.2022.127630.
Suryanarayana, C., Sudheer, C., Mahammood, V., Panigrahi, B.K., 2014. An integrated wavelet-support vector machine for groundwater level prediction in Visakhapatnam, India. Neurocomputing 145, 324–335.
Susilo, G.E., Yamamoto, K., Imai, T., 2013. Modeling groundwater level fluctuation in the tropical peatland areas under the effect of El Nino. Procedia Environmental Sciences 17, 119–128.
Swenson, S., Wahr, J., 2006. Post-processing removal of correlated errors in GRACE data. Geophys. Res. Lett. 33 (8). https://doi.org/10.1029/2005GL025285.
Tao, H., et al., 2022. Groundwater level prediction using machine learning models: a comprehensive review. Neurocomputing 489, 271–308. https://doi.org/10.1016/j.neucom.2022.03.014.
Tapley, B.D., Bettadpur, S., Watkins, M., Reigber, C., 2004. The gravity recovery and climate experiment: mission overview and early results. Geophys. Res. Lett. 31 (9). https://doi.org/10.1029/2004GL019920.
Taylor, R.G., et al., 2013. Ground water and climate change. Nat. Clim. Change 3 (4), 322–329. https://doi.org/10.1038/nclimate1744.

Thielen, D.R., et al., 2023. Effect of extreme El Niño events on the precipitation of Ecuador. Nat. Hazards Earth Syst. Sci. 23 (4), 1507–1527. https://doi.org/10.5194/nhess-23-1507-2023.

Tieleman, T., Hinton, G., 2012. Lecture 6.5-rmsprop: divide the gradient by a running average of its recent magnitude. COURSERA: Neural networks for machine learning 4 (2), 26–31.

Trenberth, K.E., 1997. The definition of el Niño. Bull. Am. Meteorol. Soc. 78 (12), 2771–2778. https://doi.org/10.1175/1520-0477(1997)078<2771:TDOENO>2.0.CO;2.

Vu, M., Jardani, A., Massei, N., Fournier, M., 2021. Reconstruction of missing groundwater level data by using Long Short-Term Memory (LSTM) deep neural network. J. Hydrol. 597, 125776.

Wada, Y., et al., 2010. Global depletion of groundwater resources. Geophys. Res. Lett. 37 (20). https://doi.org/10.1029/2010GL044571.

Wang, C., et al., 2022. Evaluation of three gridded potential evapotranspiration datasets for streamflow simulation in three inland river basins in the arid Hexi Corridor, Northwest China. J. Hydrol.: Reg. Stud. 44, 101234. https://doi.org/10.1016/j.ejrh.2022.101234.

Wang, X., et al., 2018. Short-term prediction of groundwater level using improved random forest regression with a combination of random features. Appl. Water Sci. 8 (5), 125. https://doi.org/10.1007/s13201-018-0742-6.

Wood, W.W., Imes, J.L., 2003. Dating of holocene ground-water recharge in western part of Abu Dhabi (United Arab Emirates): constraints on global climate-change models. In: Alsharhan, A.S., Wood, W.W. (Eds.), Developments in Water Science. Elsevier, pp. 379–385. https://doi.org/10.1016/S0167-5648(03)80033-3.

Woods, W.W., Imes, J.L., 1995. How wet is wet? Precipitation constraints on late Quaternary climate in the southern Arabian Peninsula. J. Hydrol. 164 (1–4), 263–268.

Wunsch, A., Liesch, T., Broda, S., 2021a. Groundwater level forecasting with artificial neural networks: a comparison of long short-term memory (LSTM), convolutional neural networks (CNNs), and non-linear autoregressive networks with exogenous input (NARX). Hydrol. Earth Syst. Sci. 25 (3), 1671–1687.

Wunsch, A., Liesch, T., Broda, S., 2021b. Groundwater level forecasting with artificial neural networks: a comparison of long short-term memory (LSTM), convolutional neural networks (CNNs), and non-linear autoregressive networks with exogenous input (NARX). Hydrol. Earth Syst. Sci. 25 (3), 1671–1687. https://doi.org/10.5194/hess-25-1671-2021.

Wunsch, A., Liesch, T., Broda, S., 2022. Feature-based groundwater hydrograph clustering using unsupervised self-organizing map-ensembles. Water Resour. Manag. 36 (1), 39–54.

Xu, G., Cheng, Y., Liu, F., Ping, P., Sun, J., 2019. A water level prediction model based on ARIMA-RNN. 2019 IEEE Fifth International Conference on Big Data Computing Service and Applications (BigDataService). IEEE, pp. 221–226.

Yang, Q., Hou, Z., Wang, Y., Zhao, Y., Delgado, J., 2015. A comparative study of shallow groundwater level simulation with WA–ANN and ITS model in a coastal island of south China. Arabian J. Geosci. 8, 6583–6593.

Yang, X., Yong, B., Ren, L., Zhang, Y., Long, D., 2017. Multi-scale validation of GLEAM evapotranspiration products over China via ChinaFLUX ET measurements. Int. J. Rem. Sens. 38 (20), 5688–5709. https://doi.org/10.1080/01431161.2017.1346400.

Yao, L., et al., 2014. Evaluation of spatial interpolation methods for groundwater level in an arid inland oasis, northwest China. Environ. Earth Sci. 71 (4), 1911–1924. https://doi.org/10.1007/s12665-013-2595-5.

Yaseen, Z.M., et al., 2016. Stream-flow forecasting using extreme learning machines: a case study in a semi-arid region in Iraq. J. Hydrol. 542, 603–614. https://doi.org/10.1016/j.jhydrol.2016.09.035.

Yin, W., Fan, Z., Tangdamrongsub, N., Hu, L., Zhang, M., 2021. Comparison of physical and data-driven models to forecast groundwater level changes with the inclusion of GRACE – a case study over the state of Victoria, Australia. J. Hydrol. 602, 126735. https://doi.org/10.1016/j.jhydrol.2021.126735.

Yoon, H., Jun, S.-C., Hyun, Y., Bae, G.-O., Lee, K.-K., 2011. A comparative study of artificial neural networks and support vector machines for predicting groundwater levels in a coastal aquifer. J. Hydrol. 396 (1), 128–138. https://doi.org/10.1016/j.jhydrol.2010.11.002.

Youssef, A.M., Pourghasemi, H.R., 2021. Landslide susceptibility mapping using machine learning algorithms and comparison of their performance at Abha Basin, Asir Region, Saudi Arabia. Geosci. Front. 12 (2), 639–655. https://doi.org/10.1016/j.gsf.2020.05.010.

Yu, P.-S., Chen, S.-T., Chang, I.F., 2006. Support vector regression for real-time flood stage forecasting. J. Hydrol. 328 (3), 704–716. https://doi.org/10.1016/j.jhydrol.2006.01.021.

Zhang, G., Zheng, W., Yin, W., Lei, W., 2020. Improving the resolution and accuracy of groundwater level anomalies using the machine learning-based fusion model in the North China plain. Sensors 21 (1), 46.

Zhang, J., Zhu, Y., Zhang, X., Ye, M., Yang, J., 2018. Developing a Long Short-Term Memory (LSTM) based model for predicting water table depth in agricultural areas. Journal of hydrology (Amsterdam) 561, 918–929. https://doi.org/10.1016/j.jhydrol.2018.04.065.

Zhang, K., et al., 2019. Parameter analysis and estimates for the MODIS evapotranspiration algorithm and multiscale verification. Water Resour. Res. 55 (3), 2211–2231. https://doi.org/10.1029/2018WR023485.